The Drakkar Group

Experiment report GDRI-DRAKKAR-2014-03-19

ORCA12.L46 climatological and interannual simulations forced with DFS4.4: GJM02 and MJM88.

Jean-Marc Molines[1], Bernard Barnier[1], Thierry Penduff[1], Anne Marie Treguier[2] and Julien Le Sommer[1]

([1]) LGGE/MEOM CNRS-UJF-OSUG, BP53, 38041 Grenoble cedex 9, France
([2]) LPO CNRS-Ifremer-IRD-UBO, BP70, 29280 Plouzané, France

March 19, 2014

Introduction

This report describes in detail the ORCA12.L46-GJM02 simulation performed in the framework of the DRAKKAR project. This run was performed during the GENCI Great Challenges 2012 on ADA, at IDRIS french HPC center. The Great Challenges offer almost no limit on CPU time for a period of 2 months during the installation and tuning of a new computer, for challenging projects. The challenge here was to run (as long as possible) an ORCA12 configuration with climatological forcing in order to (i) approach an equilibrium state and (ii) study the intrinsic variability (hence the non-forced variability) of the ocean.

A companion run (ORCA12.L46-MJM88) forced with the inter-annual forcing (whose climatology was used in GJM02) was performed on JADE at the CINES french HPC center.

For ORCA12.L46-GJM02 we were able to perform 85 years of climatological simulation, and for ORCA12.L46-MJM88 we cover the period 1958-2012 (55 years). This report is thus valid for the two simulations, given that the only difference is the forcing of the model. Additionaly, the MJM88 experiments represents the CFC^{11} during this 55-year period.

Since its completion, this long climatological simulation has already been used in publication: Treguier et al., (2014)[23]

This report is organized in different sections. The first one deals with the details of the numerical code and its parametrizations. The second section describes the model configuration, e.g. the model grid and the input data of the model. Third section deals with all forcing issues and the differences between GJM02 and MJM88 are detailed there. A fourth section is dedicated to the technical details of the production of the run and gives some informations about the computing performance. Finally, the last section gives classical elements of validation of the run, based on some of the GODAE metrics.

1 Numerical code

1.1 Overview

This experiment was performed with version 3.4 of NEMO (Madec, 2008[17]), with revision 1196 of the DRAKKAR Config Manager (DCM). CPP keys used for compilation are:

CPP key name	**Action:**
key_orca_r12=46	Define ORCA12 configuration with 46 levels
key_trabbl	Use TRAcer Bottom Boundary Layer
key_traldf_c2d	Use 2D coef for TRAcer Lateral DiFfusion
key_dynspg_flt	Use FiLTered computation for the Surface Pressure Gradient
key_dynldf_c2d	Use 2D coef for Lateral DiFfusion on the DYNamics
key_lim2	Use LIM2 ice model (default EVP rheology)
key_lim2_vp	Use LIM2 ice model with VP rheology
key_ldfslp	Compute isopycnal SLoPes for Lateral DiFfusion
key_zdftke	Use TKE closure scheme for the vertical mixing
key_zdftmx	Use tidal mixing parametrization for the vertical mixing
key_dimgout	Use DIMG binary temporary OUTput
key_mpp_mpi	Use MPP with MPI parallel code

1.2 Ocean details

1.2.1 Vertical physics

Vertical mixing :TKE scheme, EVD and tidal mixing

TKE is used to determine the vertical diffusion coefficient. The relevant namelist data are indicated below. Note that within DRAKKAR we use a non-standard treatment on ice-covered area: (a) The background avt coefficient is divided by 10 under ice. (b) The coefficient for surface input of tke (ebb) is reduced from 67.83 (open ocean) to 3.75 (ice covered regions). (c) Lang-Muir cells parametrization is turned off below ice.

In the mixing length calculation (a key variable in TKE scheme) *nn_mxl=3* is used, (the most sophisticated way for bounding the mixing length scale).

The depth of penetration of surface tke is computed using *nn_htau=1* so that it increases from 0.5m at the equator to 30m poleward of 40 degrees (standard values). Some experiments were performed in the UK (NOCS and UKMO) reducing to 10m the maximum value. A test of this modification performed with ORCA025 almost indicated a degradation (according to our standard) of the mixed layer depth in summer. Gurvan suggest that the good way to proceed is to use a map of this penetration depth, deduced from a wave monthly climatology. This is still to be done.

The vertical density instabilities are treated with enhanced vertical diffusivity (*ln_zdfevd=true*) at the interface of two layers with density inversion. In this simulation we don't apply mixing on momentum (*nn_evdm=0*). For evd mixing coefficient we use the classical value *rn_avevd=10m²/s*.

Vertical mixing produced by the tidal internal wave breaking is parameterized in the simulation (*key_zdftmx* defined). (Bessières et al., 2008[2], Koch-Larrouy et al., 2007[10]). In this simulation, the parameterization formely derived for the Indonesian Through Flow region was also applied to the Solomon Sea (as suggested by Melet et al. (2011) [19]) and to the strait of Gibraltar, as shown on figure 1.

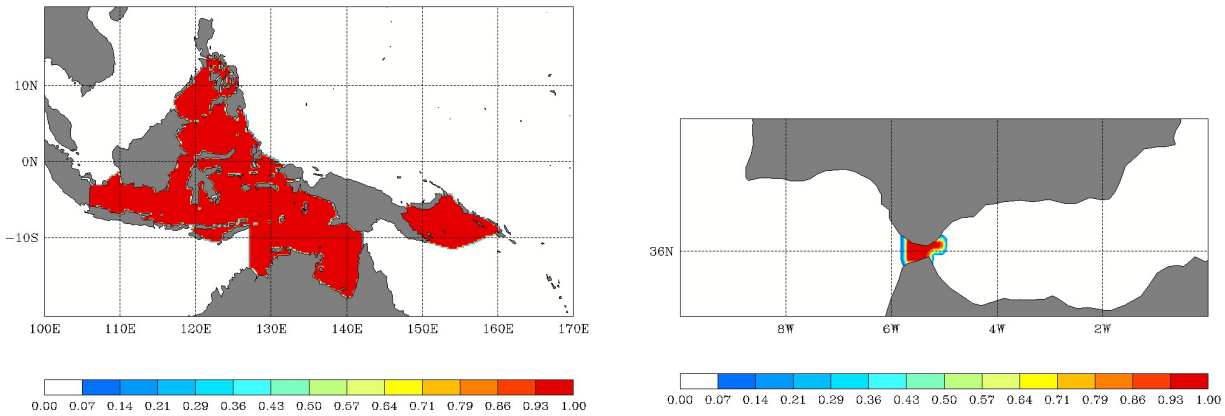

Figure 1: Extended ITF mask: Indonesian area (left) and Gibraltar Strait (right)

```
&namzdf        !   vertical physics
!-----------------------------------------------------------------------
   rn_avm0     =  1.2e-4   !  vertical eddy viscosity   [m2/s]          (background Kz if not "key_zdfcst")
```

```
   rn_avt0     =  1.2e-5   !  vertical eddy diffusivity [m2/s]          (background Kz if not "key_zdfcst")
   nn_avb      =    0      !  profile for background avt & avm (=1) or not (=0)
   nn_havtb    =    1      !  horizontal shape for avtb (=1) or not (=0)
   ln_zdfevd   = .true.    !  enhanced vertical diffusion (evd) (T) or not (F)
   nn_evdm     =    0      !  evd apply on tracer (=0) or on tracer and momentum (=1)
   rn_avevd    =  10.      !  evd mixing coefficient [m2/s]
   ln_zdfnpc   = .false.   !  Non-Penetrative Convective algorithm (T) or not (F)
   nn_npc      =    1           !  frequency of application of npc
   nn_npcp     =  365           !  npc control print frequency
   ln_zdfexp   = .false.   !  time-stepping: split-explicit (T) or implicit (F) time stepping
   nn_zdfexp   =    3           !  number of sub-timestep for ln_zdfexp=T

   ln_kzlog_wri= .false.   ! output log of kz
   ln_kztke_wri= .false.    ! output avt tke
   ln_kztid_wri= .false.    ! output avt tide
/


&namzdf_tke    !   turbulent eddy kinetic dependent vertical diffusion  ("key_zdftke")
!-------------------------------------------------------------------------
   rn_ediff    =   0.1     !  coef. for vertical eddy coef. (avt=rn_ediff*mxl*sqrt(e) )
   rn_ediss    =   0.7     !  coef. of the Kolmogoroff dissipation
   rn_ebb      =   67.83   !  coef. of the surface input of tke (67.83 now usual value)
   rn_ebbice   =   3.75    !  coef. of the surface input of tke under ice

   nn_havti    =    1      !  horizontal shape for avtb (=1) or not (=0) under ice
   rn_emin     =   1.e-6   !  minimum value of tke [m2/s2]
   rn_emin0    =   1.e-4   !  surface minimum value of tke [m2/s2]
   rn_bshear   =   1.e-20  !  background shear (>0)
   nn_mxl      =   3       !  mixing length: = 0 bounded by the distance to surface and bottom
                           !                 = 1 bounded by the local vertical scale factor
                           !                 = 2 first vertical derivative of mixing length bounded by 1
                           !                 = 3 as =2 with distinct disspipative an mixing length scale
   nn_pdl      =   1       !  Prandtl number function of richarson number (=1, avt=pdl(Ri)*avm) or not (=0, avt=avm)
   ln_mxl0     = .true.    !  surface mixing length scale = F(wind stress) (T) or not (F)
   rn_mxl0     =   0.01    !  surface  buoyancy lenght scale minimum value (0.04)
   ln_lc       = .true.    !  Langmuir cell parameterisation (Axell 2002)
   rn_lc       =   0.15    !  coef. associated to Langmuir cells
   nn_etau     =   1       !  penetration of tke below the mixed layer (ML) due to internal & intertial waves
                           !       = 0 no penetration
                           !       = 1 add a tke source below the ML
                           !       = 2 add a tke source just at the base of the ML
                           !       = 3 as = 1 applied on HF part of the stress    ("key_coupled")
   rn_efr      =   0.05    !  fraction of surface tke value which penetrates below the ML (nn_etau=1 or 2)
   nn_htau     =   1       !  type of exponential decrease of tke penetration below the ML
                           !       = 0  constant 10 m length scale
                           !       = 1  0.5m at the equator to 30m poleward of 40 degrees
/


&namzdf_tmx    !   tidal mixing parameterization                       ("key_zdftmx")
!-------------------------------------------------------------------------
   rn_htmx     = 500.      !  vertical decay scale for turbulence (meters)
   rn_n2min    = 1.e-8     !  threshold of the Brunt-Vaisala frequency (s-1)
   rn_tfe      = 0.333     !  tidal dissipation efficiency
   rn_me       = 0.2       !  mixing efficiency
   ln_tmx_itf  = .true.    !  ITF specific parameterisation
   rn_tfe_itf  = 1.        !  ITF tidal dissipation efficiency
!           !  file name            ! frequency (hours) ! variable   ! time interp. !  clim  ! 'yearly'/ ! weights  ! rotation
!           !                       !  (if <0  months)  !   name     !   (logical)  !  (T/F) ! 'monthly' ! filename ! pairing
   sn_mskitf =  'mask_itf_ORCA12_Salomon_Gibraltar'   ,      -12          , 'tmaskitf' ,   .false.    , .true. ,  'yearly' , ''
   sn_m2     =  'ORCA12_FES2012-wd' ,      -12          , 'WD_RoW_M2',   .false.    , .true. ,  'yearly' , ''       , ''
   sn_s2     =  'ORCA12_FES2012-wd' ,      -12          , 'WD_RoW_S2',   .false.    , .true. ,  'yearly' , ''       , ''
   sn_k1     =  'ORCA12_FES2012-wd' ,      -12          , 'WD_RoW_K1',   .false.    , .true. ,  'yearly' , ''       , ''
/
```

1.2.2 Horizontal physics

Tracers

As in all the DRAKKAR simulation so far, TVD advection scheme for tracer is used.

Tracer diffusion is performed with an isopycnal laplacian operator. The standard isopycnal slope computation is used. The diffusivity coefficient is proportionnal to the local grid size (it

decreases poleward) and the maximum value at the equator is 100 m^2/s, in total agreement with the value used in ORCA025 (300 m^2/s).

```
&namtra_adv    !   advection scheme for tracer
!-----------------------------------------------------------------------
   ln_traadv_cen2   =  .false.  !  2nd order centered scheme
   ln_traadv_tvd    =  .true.   !  TVD scheme
   ln_traadv_muscl  =  .false.  !  MUSCL scheme
   ln_traadv_muscl2 =  .false.  !  MUSCL2 scheme + cen2 at boundaries
   ln_traadv_ubs    =  .false.  !  UBS scheme
   ln_traadv_qck    =  .false.  !  QUICKEST scheme
/

&namtra_ldf    !   lateral diffusion scheme for tracer
!-----------------------------------------------------------------------
   !                       !  Type of the operator :
   ln_traldf_lap    =  .true.   !  laplacian operator
   ln_traldf_bilap  =  .false.  !  bilaplacian operator
   !                       !  Direction of action  :
   ln_traldf_level  =  .false.  !  iso-level
   ln_traldf_hor    =  .false.  !  horizontal (geopotential)           (require "key_ldfslp" when ln_sco=T)
   ln_traldf_iso    =  .true.   !  iso-neutral                         (require "key_ldfslp")
   ln_traldf_grif   =  .false.  !  griffies skew flux formulation     (require "key_ldfslp")
   ln_traldf_gdia   =  .false.  !  griffies operator strfn diagnostics  (require "key_ldfslp")
   ln_triad_iso     =  .false.  !  griffies operator calculates triads twice => pure lateral mixing in ML (require "key_ldfslp")
   ln_botmix_grif   =  .false.  !  griffies operator with lateral mixing on bottom (require "key_ldfslp")
                         !  Coefficient
   rn_aht_0         =  100.     !  horizontal eddy diffusivity for tracers [m2/s]
   rn_ahtb_0        =    0.     !  background eddy diffusivity for ldf_iso [m2/s]
   rn_aeiv_0        =    0.     !  eddy induced velocity coefficient [m2/s]    (require "key_traldf_eiv")
/
```

Momentum

Vector form momentum advection scheme with energy and enstrophy conserving conditions (EEN) is used. This simulation was realized before Nicolas Ducousso findings in the COMODO project. He found (1) that the lateral boundary condition along the model coast line has to be corrected and (2) that the used numerical stencil in EEN may trigger an Hollinsworth instability impacting the way eddies are generated and propagates. This will be corrected in next round of simulations.

Lateral momentum dissipation is achieved using an horizontal bi-harmonic operator. The hyper viscosity coefficient is proportional to the cube of the model grid size. The maximum value (absolute value) at the equator is $1.25^{10} m^4/s$.

```
&namdyn_adv    !   formulation of the momentum advection
!-----------------------------------------------------------------------
   ln_dynadv_vec = .true.  !  vector form (T) or flux form (F)
   ln_dynadv_cen2= .false. !  flux form - 2nd order centered scheme
   ln_dynadv_ubs = .false. !  flux form - 3rd order UBS      scheme
/

&namdyn_vor    !   option of physics/algorithm (not control by CPP keys)
!-----------------------------------------------------------------------
   ln_dynvor_ene = .false. !  enstrophy conserving scheme
   ln_dynvor_ens = .false. !  energy conserving scheme
   ln_dynvor_mix = .false. !  mixed scheme
   ln_dynvor_een = .true.  !  energy & enstrophy scheme
/

&namdyn_ldf    !   lateral diffusion on momentum
!-----------------------------------------------------------------------
   !                       !  Type of the operator :
   ln_dynldf_lap    =  .false.  !  laplacian operator
   ln_dynldf_bilap  =  .true.   !  bilaplacian operator
   !                       !  Direction of action  :
   ln_dynldf_level  =  .false.  !  iso-level
```

```
   ln_dynldf_hor    =  .true.   !  horizontal (geopotential)           (require "key_ldfslp" in s-coord.)
   ln_dynldf_iso    =  .false.  !  iso-neutral                        (require "key_ldfslp")
   !                        !  Coefficient
   rn_ahm_0_lap     = 0.        !  horizontal laplacian eddy viscosity   [m2/s]
   rn_ahmb_0        =     0.    !  background eddy viscosity for ldf_iso [m2/s]
   rn_ahm_0_blp     =  -1.25e10 !  horizontal bilaplacian eddy viscosity [m4/s]
/
```

1.2.3 Lateral boundary condition

In general, the simulation is performed with free-slip lateral boundary condition. However, for some specific areas defined in the file *shlat2d_ORCA12grid_19102011_v3.nc* (see figure 2), a no-slip or partial slip lateral boundary condition is used: in the Mediterranean Sea, in the Indonesian ThroughFlow area and in the Nares Strait (between Canada and Greenland) no-slip is applied, whereas partial slip is applied along the south-west coast of Greenland. The use of this file, prepared by Romain Bourdallé-Badie at Mercator is consensual within the ORCA12 DRAKKAR community (NOCS and GEOMAR).

```
&namlbc        !   lateral momentum boundary condition
!-----------------------------------------------------------------------
   rn_shlat    =    0.     !  shlat = 0  !  0 < shlat < 2  !  shlat = 2  !  2 < shlat
                           !  free slip  !   partial slip  !   no slip   ! strong slip
   ln_vorlat   = .false.   !  consistency of vorticity boundary condition with analytical eqs.
   ln_shlat2d  = .true.    !  use 2D file for shlat
!              !  file name      ! frequency (hours) ! variable  !time interp! clim !'yearly' !weights !rotation!
!              !                 !  (if <0  months)  !   name    !  (logical)! (T/F)!'monthly'!filename!pairing !
   sn_shlat2d = 'shlat2d_ORCA12grid_19102011_v3' , -12 , 'shlatcoef' ,.false.,.true.,'yearly' , ''     , ''
/
```

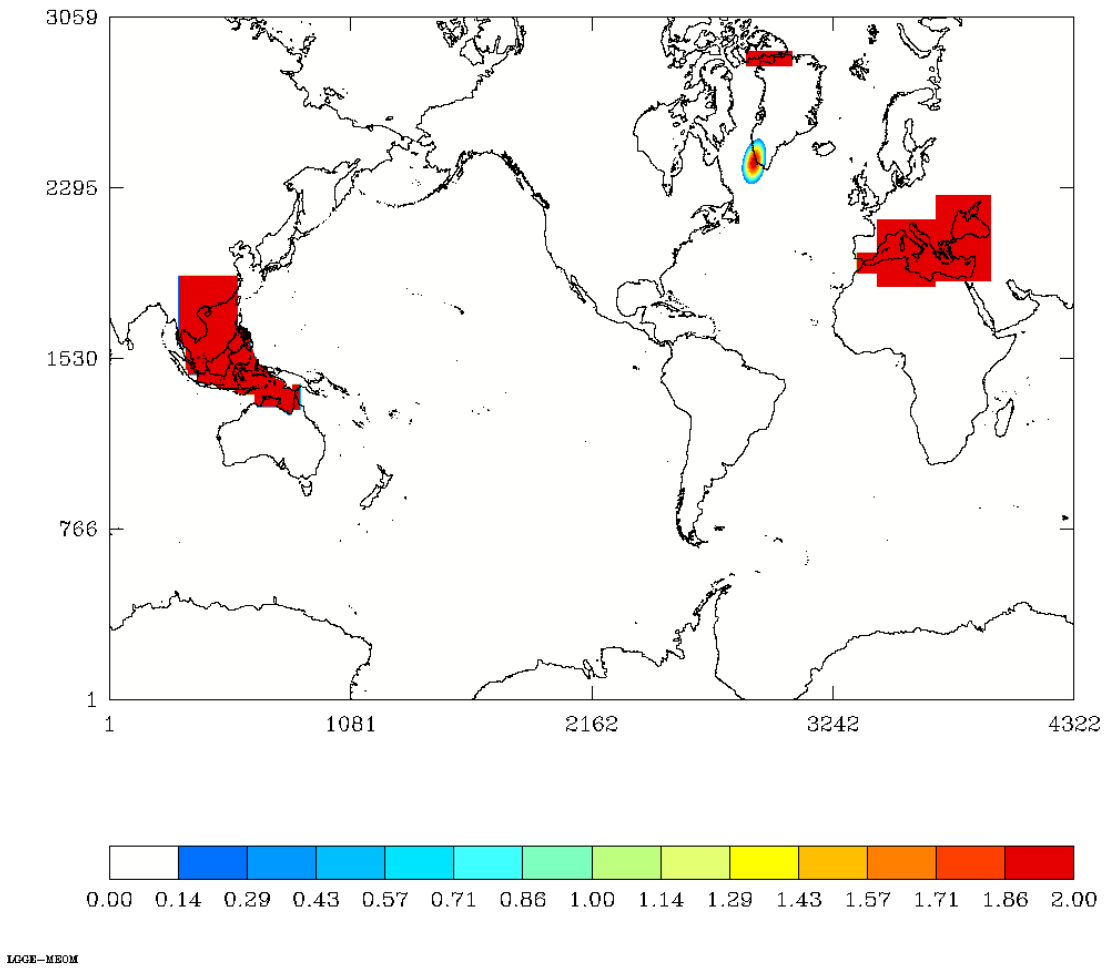

Figure 2: Lateral boundary condition as defined in shlat2d_ORCA12grid_19102011_v3.nc.

1.2.4 Bottom Boundary Layer

We used bottom boundary layer parametrization of Beckmann and Döscher (2004)[1]. Both diffusive and advective BBL parametrization is used for tracers, with Hervieux (2007)[9] improvements. There is no advective BBL for momentum.

```
&nambbl        !   bottom boundary layer scheme
!-----------------------------------------------------------------------
   nn_bbl_ldf  =  1      !  diffusive bbl (=1)   or not (=0)
   nn_bbl_adv  =  1      !  advective bbl (=1/2) or not (=0)
   rn_ahtbbl   =  1000.  !  lateral mixing coefficient in the bbl  [m2/s]
   rn_gambbl   =  10.    !  advective bbl coefficient                [s]
   ln_kriteria = .true.  !  activate BBL on k-criteria instead of depth criteria
/
```

1.2.5 Bottom Friction

A classical quadratic bottom friction is used, with a drag coefficient of rn_bfri2=1.e-3 m^2/s^2. An enhanced bottom friction was applied over the Bering Strait and over the Torres Strait (respectively left and right on figure 3). The enhanced bottom friction mask ($bfrcoef2d$) is

read in the file orca12_bfr_coef_MAL101.nc). Then, the 2D drag coefficient is computed this way :
$bfrcoef2d(:,:) = rn\_bfri2 * (1 + rn\_bfrien * bfrcoef2d(:,:))$
In this simulation the amplification factor (rn_bfrien) is set to 50, which imply the use of an implicit scheme for stability reasons.

```
&nambfr        !   bottom friction
!-----------------------------------------------------------------------
   nn_bfr      =    2      !  type of bottom friction :   = 0 : free slip,  = 1 : linear friction
                           !                              = 2 : nonlinear friction
   rn_bfri1    =    4.e-4  !  bottom drag coefficient (linear case)
   rn_bfri2    =    1.e-3  !  bottom drag coefficient (non linear case)
   rn_bfeb2    =    2.5e-3 !  bottom turbulent kinetic energy background  (m2/s2)
   ln_bfr2d    = .true.    !  horizontal variation of the bottom friction coef (read a 2D mask file )
   rn_bfrien   =    50.    !  local multiplying factor of bfr (ln_bfr2d=T)
   ln_bfrimp   = .true.    !  implicit bottom friction (requires ln_zdfexp = .false. if true)
/
```

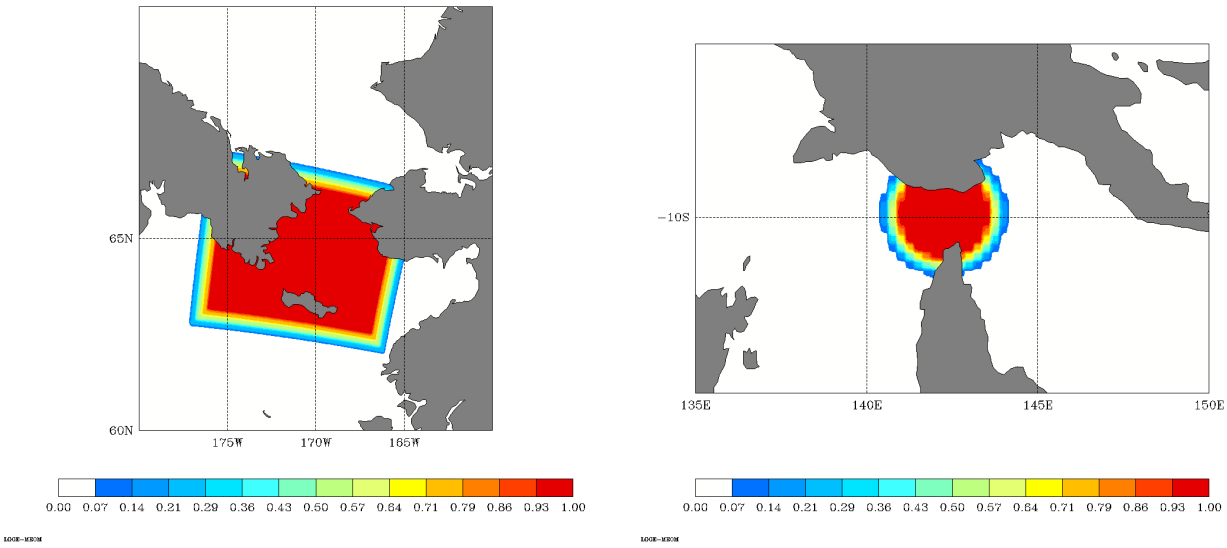

Figure 3: Bottom friction enhancement coefficient: Bering Strait (left) and Torres Strait (right)

1.2.6 Tracer damping strategy

The tracer damping strategy is common to all our DRAKKAR runs (nn_hdmp=-2). Although the idea is to keep tracer damping as reduced as possible, it is necessary to have it in order to address the following 3 identified problems :
(1) Fix tracer trends in almost closed seas where the forcing is not trusted, (2) fix spurious modification of water mass properties downstream of overflow regions and (3) reduce the long term trend in ACC transport, linked to the decrease of AABW volume.

Additionally, in the climatological run, we do observed the formation of a spurious polynia in the center of the Weddell Sea and as a consequence, a very deep convection (almost to the bottom) there, that drastically changed the properties of the deep waters. Many tests were performed (see section 4) aiming at eliminating the polynia, but none worked satisfactory, except having a light TS restoring in the upper ocean. Due to the production context of the GENCI "grand challenge", with very short available production time, we opt for keeping this light restoring.

The Gouretski and Koltermann (2004) annual climatology is used; this climatology, build with isopycnal interpolation previous the regridding on z-level is prefered to the standard Levitus climatology, especially for the Southern Ocean, were spurious density inversion in Levitus

are noticeable.
In the DRAKKAR version of *tradmp.F90*, *resto* subroutine has been modified so that the definitions of the restoring zones are independant of the model configuration and are given in geographical coordinates either as a rectangular shape or as a circular shape with localized center and given radius, associated with a depth range. This helps in maintaining a coherent strategy for all the DRAKKAR configurations.

In the following paragraphs some details on the implementation of the tracer damping for the three points mentioned above, are given:

Regional 3D damping (semi-enclosed seas)
Table 1 gives the characteristics of the 3D TS damping zones.

Region	Longitude Range	Latitude Range	Depth Range(m)	time scale (d)
Red Sea	29.4 E - 43.6 E	12.9 N - 30.3 N	0. - bottom	180.
Black Sea	27.4 E - 42.0 E	41.0 N - 47.5 N	0. - bottom	180.
Persian Gulf	46.5 E - 57.0 E	23.0 N - 31.5 N	0. - bottom	180.

Table 1: Definition of 3D TS restoring zone.

Downstream the overflows and Weddell Sea polynia fix
One of the major flaws of the numerical model is its incapacity of well representing the overflow of dense waters over sills, despites the BBL parameterization. As a consequence of this flaw, the entrainement downstream the sill is far too much, leading to produce a too light (hence too shallow) overflow water.

This effect is particularly dramatic for the mediterranean outflow at Gibraltar Strait: without damping, in general the Med Sea Water (MW) spreads out at 450-500m whereas it should get deep to 1200 m. After years of simulations, this has a huge impact on the water masses of the North Atlantic, which is not acceptable. In ORCA12.L46-MAL101 simulation, we found that at this resolution and with a precise local bathymetry, that preserves a natural submarine canyon, we were able to significantly improve the quality (both in depth and density) of the MW overflow, but with the climatological forcing, (this run) it appeared that for a long integration it was not enough and we did not take the risk of "poluting" all the North Atlantic. Other similar regions such as Bab-el-Mandeb (conexion between the Red Sea and the Gulf of Aden) and Ormuz Strait (conexion between the Persian Gulf and the Arabian Sea) should behave in an almost similar way and the same restoring strategy is used there.

The overflow of the Nordic Seas at Denmark strait and Faroes Bank channel, cannot be fixed so drastically, because on long term run, the interannual variability (which is one of our scientific interest) may be driven by the variability of the overflow, which is killed by the TS restoring process.
Table 2 gives the characteristics of the overflow damping zone.

Antarctic Bottom Water restoring
In order to reduce the ACC trend (transport slowly decreasing, associated with the consumption of AABW), an *ad hoc* 3D TS restoring (time scale of 2 years) is applied in the Southern

Region	Center	Radius (km)	Depth Range(m)	time scale (d)
Gibraltar Strait	7.0 W - 36.0 N	80	600 - 1300	6.
Bab-el-Mandeb	44.75 E - 11.5 N	100	0 - bottom	6.
Ormuz Strait	57.75 E - 25.0 N	100	0 - bottom	6.
	Longitude Range	**Latitude Range**	**Depth Range(m)**	**time scale (d)**
Weddell Sea	66 W - 15.0 E	75.0 S - 60.0 S	0. - 500	360.

Table 2: Definition of regional patches for overflow and polynia issues.

Ocean (Dufour, 2011 ([6], and Dufour et al., 2012 [7]) The restoring is applied in an area limited by the $\sigma_2 = 34.7$ isopycnal, a depth greater than 1000m and south of 30S. The file giving the damping mask is *ORCA12.L46_ dmp_ mask.nc*, and it has been created with *cdfmaskdmp* CDFTOOL using T/S Gouretski climatology 2004. On figure 4, horitontal maps of the damping mask are given for depths around 2000 and 3000mas well as a meridional section of the mask at 30W. Note that the transition between the zone of restoring and the 'free' ocean is smooth. In the future we may think of a more abrupt transition. Where the coefficient is 1, the restoring time scale is 2 years. For 0.1, it is increased to 20 years. The issue of a more abrupt transition is mainly to short cut long discussions with hair-splitting reviewers !

```
&namtra_dmp    !   tracer: T & S newtonian damping
!-----------------------------------------------------------------------
   ln_tradmp   =  .true.    !  add a damping termn (T) or not (F)
   nn_hdmp     =   -2       !  horizontal shape =-1, damping in Med and Red Seas only
                            !                   =XX, damping poleward of XX degrees (XX>0)
                            !                      + F(distance-to-coast) + Red and Med Seas
                            !                   =-2, DRAKKAR customization
   nn_zdmp     =    0       !  vertical   shape =0    damping throughout the water column
                            !                   =1 no damping in the mixing layer (kz  criteria)
                            !                   =2 no damping in the mixed  layer (rho crieria)
   rn_surf     =   50.      !  surface time scale of damping   [days]
   rn_bot      =  360.      !  bottom  time scale of damping   [days]
   rn_dep      =  800.      !  depth of transition between rn_surf and rn_bot [meters]
   nn_file     =    0       !  create a damping.coeff NetCDF file (=1) or not (=0)
   ln_dmpmask  = .true.     !  Read dmp_mask.nc file  when T (between 0 and 1 )
   rn_timsk    =  730.      !  Time scale used for dmp_mask
/

&namtsd    !   data : Temperature  & Salinity
!-----------------------------------------------------------------------
!          ! file name ! frequency (hours)    ! variable ! time interp. ! clim  !'yearly' or ! weights  ! rotation !
!          !           !  (if <0  months)     !   name   !  (logical)   ! (T/F) ! 'monthly'  ! filename ! pairing  !
   ! data used for initial condition (istate)
   sn_tem_ini  = 'Levitus_p2.1_1m_01_12_Tpot_mms025_ORCA_R12'     , -1,'votemper',  .true.  , .true., 'yearly'   , ' ' , ' '
   sn_sal_ini  = 'Levitus_p2.1_1m_01_12_S_correc_mms025_ORCA_R12' , -1,'vosaline',  .true.  , .true., 'yearly'   , ' ' , ' '
   ! data used for damping ( tradmp)
   sn_tem_dmp  = 'Gouretski_ANNUAL_T_orca12.l46-MAL101_blk_sea_cor'   , -12, 'votemper',  .false.  , .true., 'yearly'   , ' ' ,
   sn_sal_dmp  = 'Gouretski_ANNUAL_S_orca12.l46-MAL101_blk_sea_cor'   , -12, 'vosaline',  .false.  , .true., 'yearly'   , ' ' ,
   !
   cn_dir        = './'     !  root directory for the location of the temperature and salinity file
   ln_tsd_init   = .true.   !  Initialisation of ocean T & S with T &S input data (T) or not (F)
   ln_tsd_tradmp = .true.   !  damping of ocean T & S toward T &S input data (T) or not (F)
/
```

2 Model configuration

2.1 Bathymetry

The bathymetry used for this simulation (*bathymetry_ ORCA12_ V3.3.nc*) is a merge of etopo1 (1') for the deep ocean and gebco08 (30") for shallow areas (+ plug base10 (30") on the European coast). Then coast line and some hand modifications were applied (see Bourdallé-Badie

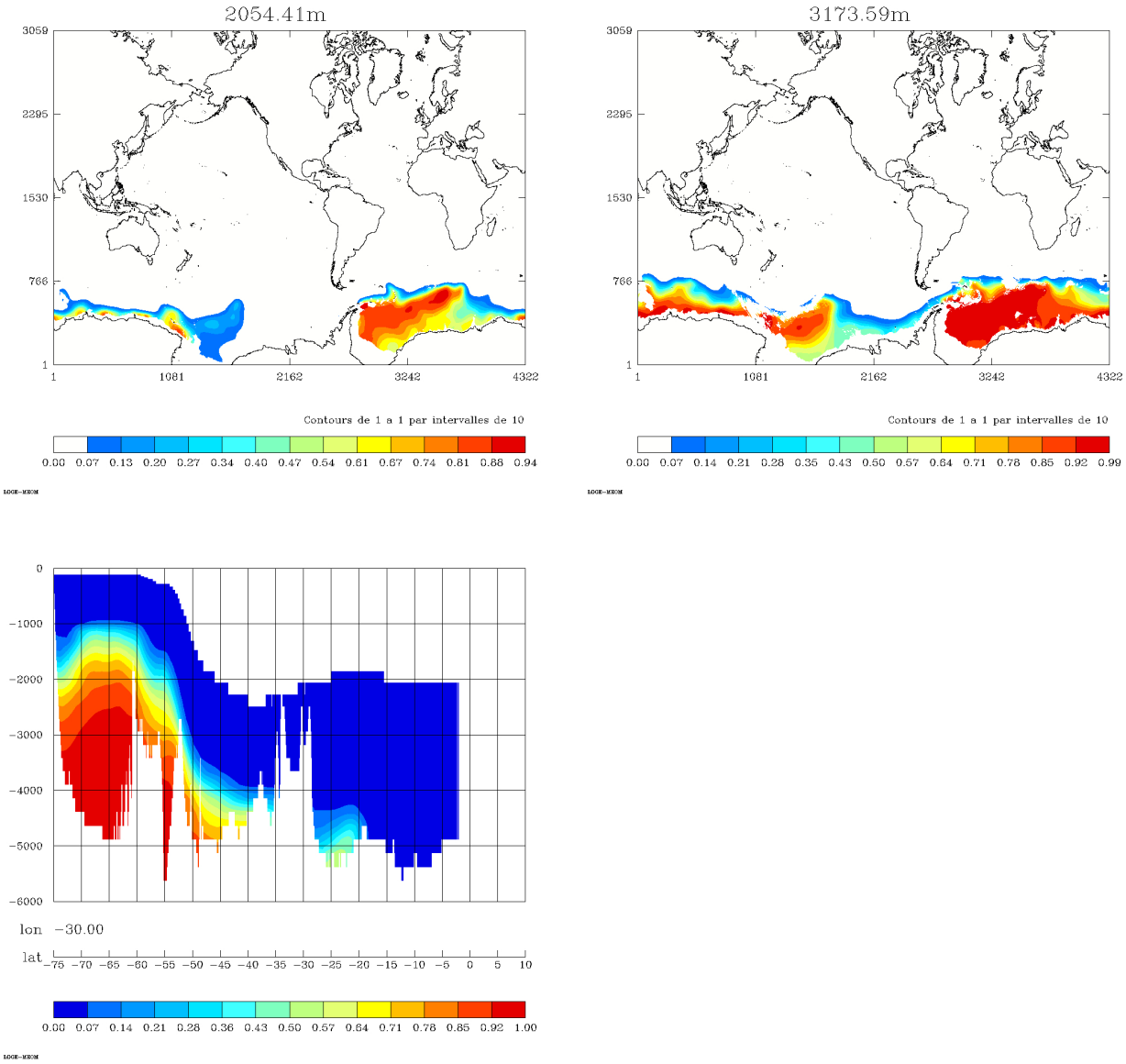

Figure 4: AABW damping mask at 2000m, 3000m (upper panel from left to right) and section at 30W (lower panel)

et al, 2012 [3] for details.)

This V3.3 bathymetry file is the same as V3.2 described in [3] except that Amery Ice Shelf was removed because it was only one grid point wide in ORCA12 configuration. On figure 6 this weird and rather suspicious stripe of water, near the periodic folding line of the grid is shown.

Figure 5 shows the location of Amery Ice Shelf and on figure 6 this weird and rather suspicious stripe of water, near the periodic folding line is clearly visible for bathymetry V3.2.

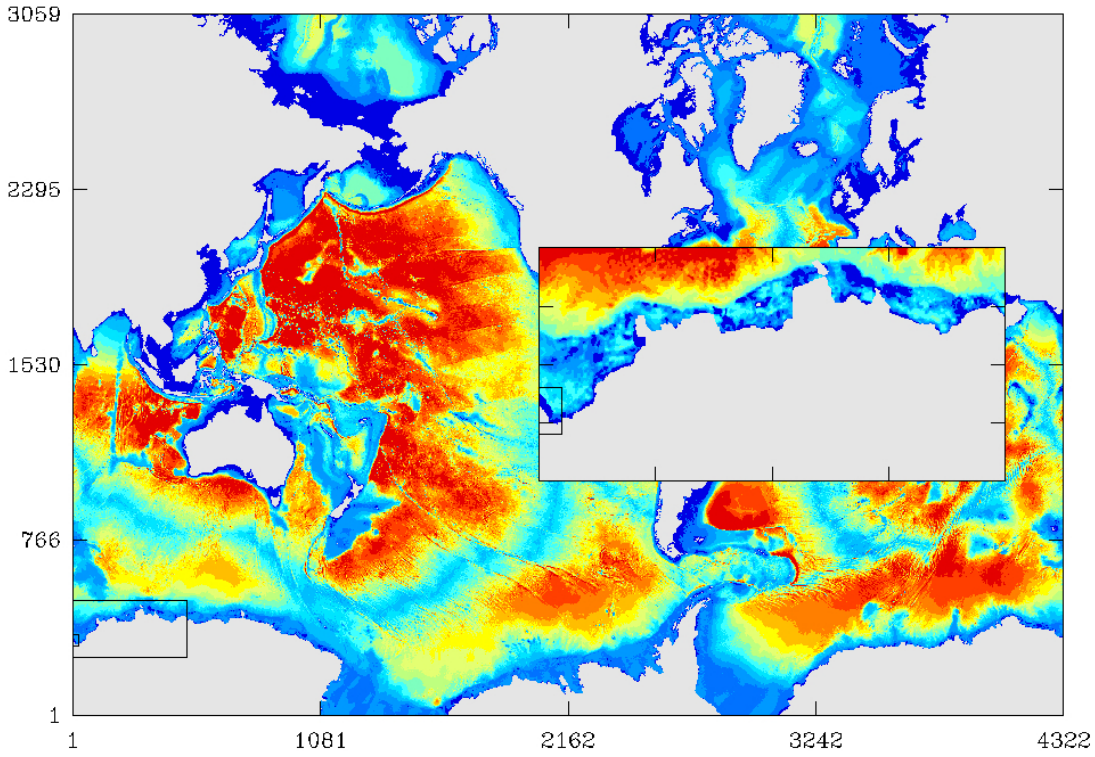

Figure 5: Global ORCA12 bathymetry with localisation of Amery Ice Shelf.

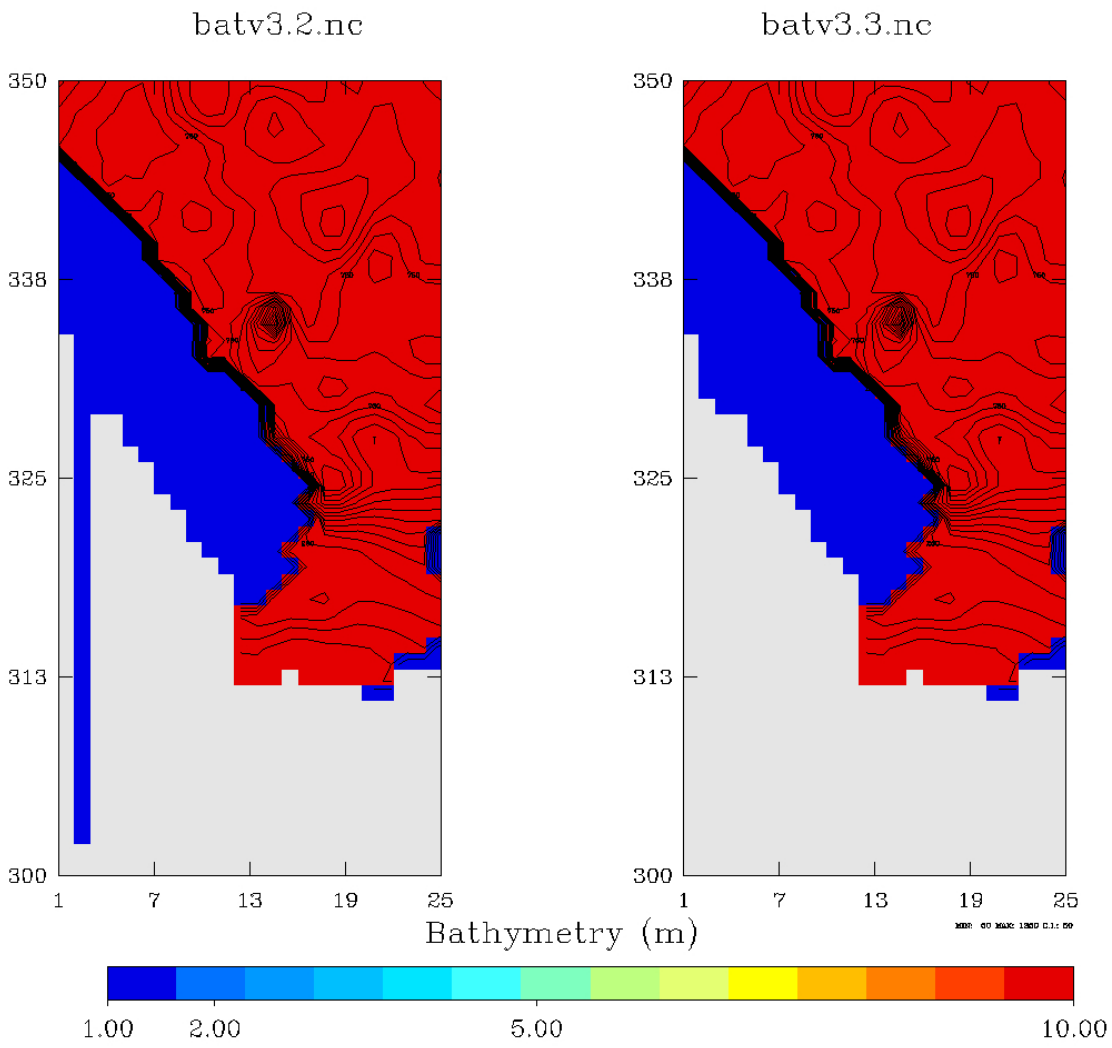

Figure 6: Bathymetry v3.2 and v3.3 in the region of Amery Ice Shelf.

In the *bathymetry_ORCA12_V3.3.nc* file, the minimum depth is set to 1m, but when running the model, there are always at least 3 vertical levels (*nn_hmin=-3*), and with the partial steps settings in use, this leads to a real minimum depth in the model of 14.5 m. Closed seas as well as lakes are removed. This bathymetric file (v3.3) is used nowadays by the ORCA12 DRAKKAR community (FR, NOCS and GEOMAR).

```
&namdom        !   space and time domain (bathymetry, mesh, timestep)
!-----------------------------------------------------------------------
   nn_bathy    =    1      !  compute (=0) or read (=1) the bathymetry file
   nn_closea   =    0      !  remove (=0) or keep (=1) closed seas and lakes (ORCA)
   nn_msh      =    0      !  create (/=0) a mesh file(s) or not (=0)
                           !  if not 0 can be in [1 - 6 ] for drakkar usually 6
   rn_hmin     =   -3.     !  min depth of the ocean (>0) or min number of ocean level (<0)
   rn_e3zps_min=   25.     !  partial step thickness is set larger than the minimum of
   rn_e3zps_rat=    0.2    !  rn_e3zps_min and rn_e3zps_rat*e3t, with 0<rn_e3zps_rat<1
                           !
   rn_rdt      =  480.     !  time step for the dynamics (and tracer if nn_acc=0)
   nn_baro     =   60      !  number of barotropic time step            ("key_dynspg_ts")
   rn_atfp     =    0.1    !  asselin time filter parameter
   nn_acc      =    0      !  acceleration of convergence : =1      used, rdt < rdttra(k)
                           !                                =0, not used, rdt = rdttra
   rn_rdtmin   =  480.     !  minimum time step on tracers (used if nn_acc=1)
   rn_rdtmax   =  480.     !  maximum time step on tracers (used if nn_acc=1)
   rn_rdth     =  800.     !  depth variation of tracer time step  (used if nn_acc=1)
/
```

2.2 Horizontal grid

The horizontal grid is the standard ORCA12 tri-polar grid (4322 x 3059 grid points). The 1/12° resolution corresponds to the equator (10km). Resolution increases poleward: 5km at 60°, 3.5km at 75° (except in the Arctic Ocean, the grid size is scaled by the cosine of the latitude. This mesh requires the use of a North Pole folding condition which has been largely improved in terms of performance in the recent versions of NEMO.

2.3 Vertical grid

The vertical grid uses the 46 DRAKKAR standard levels, as described in table 3.

level	gdept	gdepw	e3t	e3w
1	3.05	0.00	6.19	6.00
2	9.45	6.19	6.64	6.40
3	16.36	12.84	7.20	6.90
4	23.90	20.04	7.89	7.53
5	32.21	27.95	8.76	8.30
6	41.48	36.71	9.83	9.26
7	51.95	46.55	11.15	10.45
8	63.88	57.71	12.78	11.92
9	77.62	70.50	14.78	13.73
10	93.59	85.30	17.24	15.95
11	112.28	102.56	20.24	18.66
12	134.28	122.83	23.88	21.97
13	160.28	146.74	28.26	25.97
14	191.09	175.03	33.51	30.77
15	227.62	208.58	39.72	36.49
16	270.90	248.35	47.01	43.23
17	322.02	295.40	55.43	51.07
18	382.14	350.88	65.02	60.08
19	452.44	415.95	75.76	70.25
20	534.02	491.76	87.56	81.54
21	627.85	579.35	100.24	93.80
22	734.72	679.62	113.57	106.84
23	855.11	793.20	127.25	120.39
24	989.23	920.46	140.96	134.12
25	1136.92	1061.40	154.35	147.71
26	1297.72	1215.73	167.13	160.83
27	1470.89	1382.82	179.05	173.21
28	1655.47	1561.82	189.93	184.62
29	1850.37	1751.70	199.67	194.94
30	2054.41	1951.32	208.24	204.10
31	2266.45	2159.51	215.66	212.09
32	2485.37	2375.12	222.00	218.96
33	2710.13	2597.08	227.37	224.80
34	2939.81	2824.41	231.85	229.71
35	3173.59	3056.23	235.58	233.81
36	3410.76	3291.79	238.65	237.19
37	3650.71	3530.42	241.17	239.98
38	3892.95	3771.57	243.23	242.26
39	4137.05	4014.79	244.90	244.11
40	4382.65	4259.68	246.26	245.62
41	4629.48	4505.93	247.36	246.84
42	4877.30	4753.28	248.25	247.83
43	5125.92	5001.52	248.96	248.62
44	5375.18	5250.48	249.53	249.26
45	5624.95	5500.01	250.00	249.78
46	5875.14	5750.00	250.37	250.19

Table 3: Vertical levels and vertical metrics used in the simulation

2.4 Initial conditions

2.4.1 Ocean

The model started at rest, with initial temperature and salinity conditions taken from a monthly climatology. The used climatology is a merge of the Levitus 1998 climatology, patched with PHC2 for the Arctic regions and Medatlas for the Mediterranean Sea. For this simulation, the climatology was regridded on ORCA12 3D grid. Some adjustments were necessary for the deeper layers where spurious very low salinities showed up which made the model blow up. This kind of problem was already identified in previous run and configuration. It is likely due to a mismatch of the Levitus original bottom topography and the bathymetry of higher resolution model. Therefore, no easy fix was found to work around this problem, definitively. Mercator-Ocean proposed to have a well debugged climatology on the ORCA05 grid, and use

it in all configuration with interpolation on the fly and *ad hoc* weight files. This is worth to be tried !

2.4.2 Ice

Initial condition for ice (ice concentration, ice thickness) was taken from a previous ORCA12.L46 run, (MAL101 configuration) using the January monthly climatology computed over the period 1998-2007. The file used for this purpose is *ORCA12.L46-MAL95_y1998-2007m01_icemod_initMAL101.n*
MAL101 was itself initialized from MAL95 10 year January climatology. At the end, MAL95 was a continuation of K001 run started in 1978 with CORE forcing and default standard initial ice conditions.
The ice concentration and thickness exhibit a strong annual cycle which is recovered after only few years of integration. However, a long term climatic trend is clearly visible and very well correlated with observations, in particular in the Arctic Ocean. So it is quite clear that the state of the sea-ice in the 2010's is very different from the state in the late 1950's. Therefore, should we think about a more clever way of performing ice initialisation ? For reference, the actual ice initial condition and the BOOTSTRAP product are shown on figure 7.

```
&namiceini     !   ice initialisation
!-----------------------------------------------------------------------
   ln_limini   = .true.   !  read the initial state in 'Ice_initialization.nc' (T) or not (F)
   ttest       =  2.0     !  threshold water temperature for initial sea ice
   hninn       =  0.5     !  initial snow thickness in the north
   hginn       =  1.0     !  initial ice  thickness in the north
   alinn       =  0.05    !  initial leads area     in the north
   hnins       =  0.1     !  same  three parameter  in the south
   hgins       =  1.0     !        "                "     south
   alins       =  0.1     !        "                "     south
/
```

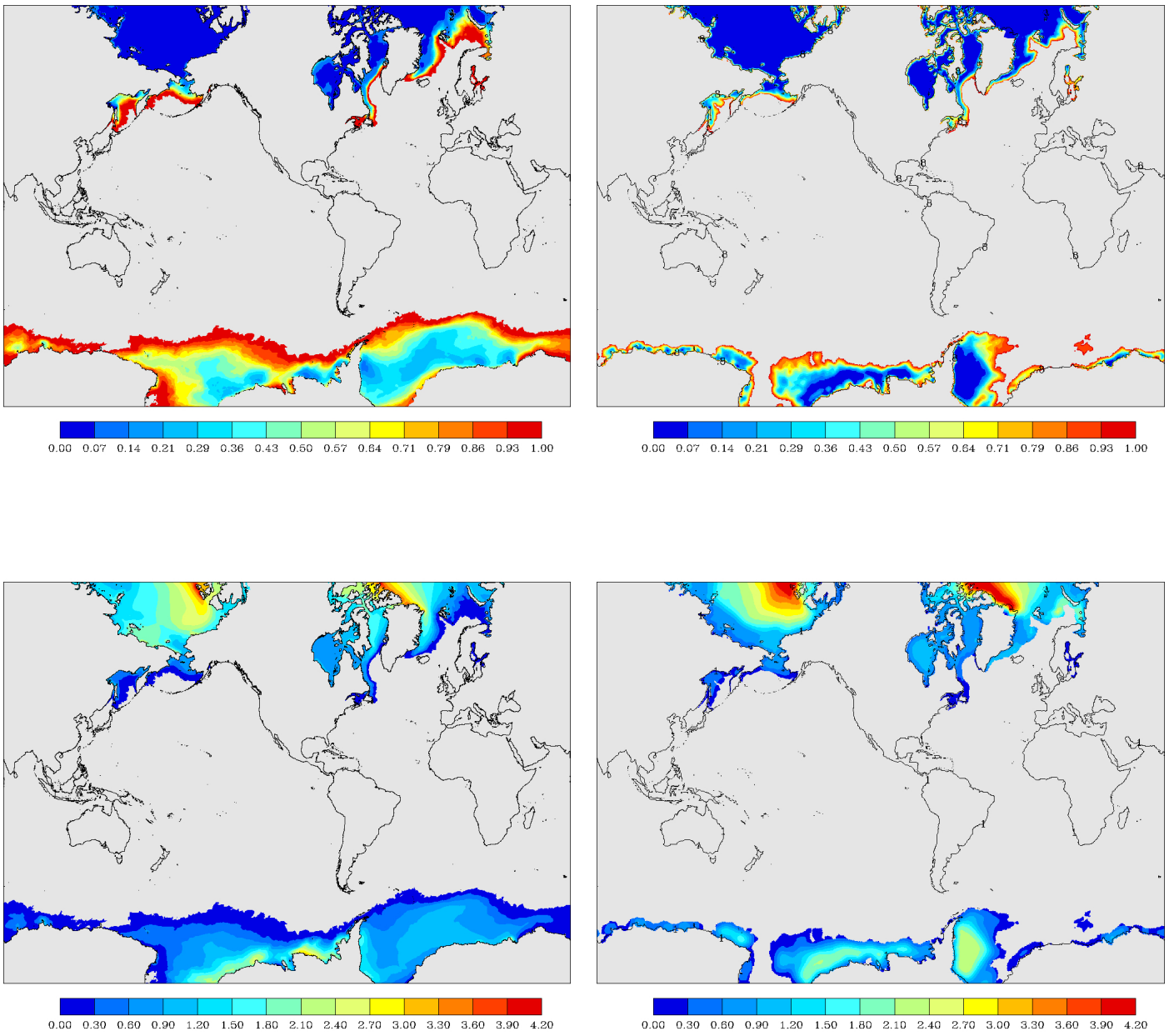

Figure 7: Comparison of the ice initialisation use in ORCA12.L46-GJM02 (left) and the Bootstrap product for January 1989(right). Upper row shows lead fraction, lower row shows ice thickness

2.5 Miscellaneous

Once in production the model is stable with a time step of 480 seconds. However, during the first month of production, time-step was increased from 72 seconds to 480 seconds. Details of the initial procedure are given in section 4.

3 Forcing the model: Surface Boundary Conditions

3.1 CORE Bulk formulae

Since the very beginning of the DRAKKAR project, the CORE bulk formulae (Large & Yeager, 2004 [11]) have been used in the configurations. With these formulae, sensible and latent heat fluxes are computed as well as evaporation and wind stresses. In the same routine, for the sake of simplicity, radiative fluxes (solar and non-solar) and precipitations (total and solid), are processed in order to provide a complete surface boundary condition (SBC) to the ocean and ice models. CORE bulk formulae take 8 (+1) different atmospheric fields as input:

Turbulent variables : 2m temperature (t2), 2m humidity (q2), 10m zonal wind velocity (u10) and 10m meridional wind velocity (v10).

Radiative fluxes : Solar downward (or short-wave) radiative flux, Non-solar downward (or Infra-red, or long-wave) radiative flux.

Fresh water input : Total precipitation, and solid precipitation (snow). The convention is to use upward fresh water fluxes, so that

Total Cloud Cover : This field is not part of the CORE bulk formulae, but in this particular simulation, it has been used in place of constant values. This variable in only used in the ice model, in order to compute a parameter influencing the solar radiation penetration into the ice. No evaluation of the impact of this variable has been done so far.

This general DRAKKAR strategy is valid for the interannual simulations.
In case of climatological simulation (which is the case for GJM02), some adaption are made in the input field, in order to correctly represent the non-linear terms. In the bulk formulae, the wind speed is used $wnd = \sqrt{U^2 + V^2}$ in the computation of exchange coefficients (C_d, C_e, C_h) and in the wind stress components $\tau_x = C_d \cdot wnd \cdot U$, $\tau_y = C_d \cdot wnd \cdot V$ For the climatological run the climatology of the wind speed as well as the climatology of the pseudo-stress ($wnd \cdot U$, $wnd \cdot V$) are computed and used directly in the formulae. Doing so, most of the non linear terms of the bulk formulae are preserved, and comparision with inter-annualy forced run is relevant.

To be more precise, in the above formulae, U and V represent an estimation of the surface wind components. They are generally computed using the difference between 10m wind components (u_{10} and v_{10}) and the ocean surface velocity ($u_{oce}(1)$, $v_{oce}(1)$) ('relative wind forcing') so that, $U = (u_{10} - u_{oce}(1))$, $V = (v_{10} - v_{oce}(1))$. In DRAKKAR, an alternative is possible having just $U = u_{10}$ and $V = v_{10}$ ('absolute wind forcing'). The two different ways of computing the estimation of surface wind, give big differences, in particular in the Eddy Kinetic Energy of the upper ocean, absolute wind forcing giving higher (and more realistic –compared to satellite estimates –) EKE. In this run, as far as a climatological forcing is used, the pseudo stress is computed without information from the ocean surface currents, and the 'absolute wind forcing' is natural. For the coherency of the 2 simulations, it was used as well in the inter-annual run.

3.2 DFS4.4 atmospheric data set

In this simulation, DFS4.4 atmospheric fields are used. This Drakkar Forcing Set is based on ERA40 ECMWF reanalysis from 1958 to 2001 and on ERAinterim ECMWF reanalysis from 2002 to 2012. In fact, for the ERA40 period, DFS4.4 is strictly identical to DFS4.3 (Brodeau et al., 2009 [4]). For the ERAinterim period, a particular treatment has been performed in order to avoid unrealistic jumps at the end of 2001. ERAinterim fields have been rescaled to ensure

continuity, and the variables were re-mapped on ERA40 grid. The frequencies where also made similar to those of DFS4.3. Therefore, in DFS4.4 turbulent variables are given every 6 hours, radiative fluxes every day and precipitation every month.

The climatological forcing was computed as the daily average for the whole DFS4.4 period, from 1958 to 2012. For the climatological run, daily turbulent variables (wnd10, wu10 and wv10) are used instead of 6-hourly. Radiative fluxes are still daily and precip/snow still monthly.

The forcing routine and the ice model are called only every *nn_fsbc=4* time-step in order to save computing time. When the model runs in production mode, time step is *nn_rdt=480s*, so that the forcing and ice model are called 45 times in 24h (every 32 mn), which seems to be sufficient, with regard to the highest frequency in the forcing variables (6 hrs). A detailed description of the DFS forcings is available in Dussin et al. (2014)[21].

```
&namsbc        !   Surface Boundary Condition (surface module)
!------------------------------------------------------------------------
   nn_fsbc     = 4         !  frequency of surface boundary condition computation
                           !     (also = the frequency of sea-ice model call)
   ln_ana      = .false.   !  analytical formulation                    (T => fill namsbc_ana )
   ln_flx      = .false.   !  flux formulation                          (T => fill namsbc_flx )
   ln_blk_clio = .false.   !  CLIO bulk formulation                     (T => fill namsbc_clio)
   ln_blk_core = .true.    !  CORE bulk formulation                     (T => fill namsbc_core)
   ln_blk_mfs  = .false.   !  MFS bulk formulation                      (T => fill namsbc_mfs )
   ln_cpl      = .false.   !  Coupled formulation                       (T => fill namsbc_cpl )
   ln_apr_dyn  = .false.   !  Patm gradient added in ocean & ice Eqs.   (T => fill namsbc_apr )
   nn_ice      = 2         !  =0 no ice boundary condition   ,
                           !  =1 use observed ice-cover      ,
                           !  =2 ice-model used                         ("key_lim3" or "key_lim2)
   ln_dm2dc    = .true.    !  daily mean to diurnal cycle on short wave
   ln_rnf      = .true.    !  runoffs                                   (T => fill namsbc_rnf)
   ln_ssr      = .true.    !  Sea Surface Restoring on T and/or S       (T => fill namsbc_ssr)
   nn_fwb      = 0         !  FreshWater Budget: =0 unchecked
                           !     =1 global mean of e-p-r set to zero at each time step
                           !     =2 annual global mean of e-p-r set to zero
                           !     =3 global emp set to zero and spread out over erp area
   ln_cdgw = .false.       !  Neutral drag coefficient read from wave model (T => fill namsbc_wave)
/
```

```
&namsbc_core   !   namsbc_core  CORE bulk formulae  *** ORCA12.L46-GJM02 ***
!-----------------------------------------------------------------------
!             !  file name         ! frequency (hours) ! variable  ! time interp. !  clim  ! 'yearly'/ ! weights  ! rotation !
!             !                    !  (if <0  months)  !   name    !   (logical)  !  (T/F) ! 'monthly' ! filename ! pairing  !
   sn_wu   =    'drowned_wu10_DFS4.4_CLIM_0001' ,    24 ,  'wu10'   ,    .true.    , .true. , 'yearly' ,  'wght_bicub_ERA40_ORCA12.nc'  , 'U1'
   sn_wv   =    'drowned_wv10_DFS4.4_CLIM_0001' ,    24 ,  'wv10'   ,    .true.    , .true. , 'yearly' ,  'wght_bicub_ERA40_ORCA12.nc'  , 'V1'
   sn_wnd  =    'drowned_w10_DFS4.4_CLIM_0001'  ,    24 ,  'w10'    ,    .true.    , .true. , 'yearly' ,  'wght_bilin_ERA40_ORCA12.nc'  ,  ''
   sn_qsr  =    'radsw_DFS4.4_nofilt_y1958-2010' ,   24 ,  'radsw'  ,    .false.   , .true. , 'yearly' ,  'wght_bilin_NCAR_ORCA12.nc' ,  ''
   sn_qlw  =    'drowned_radlw_DFS4.4_CLIM_0001' ,   24 ,  'radlw'  ,    .false.   , .true. , 'yearly' ,  'wght_bilin_NCAR_ORCA12.nc' ,  ''
   sn_tair =    'drowned_t2_DFS4.4_CLIM_0001'   ,    24 ,  't2'     ,    .true.    , .true. , 'yearly' ,  'wght_bilin_ERA40_ORCA12.nc' ,  ''
   sn_humi =    'drowned_q2_DFS4.4_CLIM_0001'   ,    24 ,  'q2'     ,    .true.    , .true. , 'yearly' ,  'wght_bilin_ERA40_ORCA12.nc' ,  ''
   sn_prec =    'drowned_precip_DFS4.4_CLIM_0001' ,  -1 ,  'precip' ,    .true.    , .true. , 'yearly' ,  'wght_bilin_NCAR_ORCA12.nc' ,  ''
   sn_snow =    'drowned_snow_DFS4.4_CLIM_0001' ,    -1 ,  'snow'   ,    .true.    , .true. , 'yearly' ,  'wght_bilin_NCAR_ORCA12.nc' ,  ''
   sn_tdif =    ' '                            ,    24 ,  'taudif' ,    .true.    , .true. , 'yearly' ,  ''                                                    ,  ''
   sn_ccov =    'drowned_tcc_ERAinterim_1y_CLIM' ,  -12 , 'tcc'    ,    .false.   , .true. , 'yearly' ,  'wght_bilinear_DFS5-ORCA12_flip.nc'  ,  ''

!
   cn_dir      = './'      !  root directory for the location of the bulk files
   ln_2m       = .true.    !  air temperature and humidity referenced at 2m (T) instead 10m (F)
   ln_taudif   = .false.   !  HF tau contribution: use "mean of stress module - module of the mean stress" data
   rn_pfac     = 1.00      !  multiplicative factor for precipitation (total & snow)

   ln_kata     = .false.    ! katabatic wind enhancement
!             !  file name                  ! frequency (hours) ! variable  ! time interp. !  clim  ! 'yearly'/ ! weights  ! rotation !
!             !                             !  (if <0  months)  !   name    !   (logical)  !  (T/F) ! 'monthly' ! filename ! pairing  !
   sn_kati     =     'katamask'     ,      -1           , 'katamaskx',    .false.     , .true.  ,  'yearly'  , ''       , ''
   sn_katj     =     'katamask'     ,      -1           , 'katamasky',    .false.     , .true.  ,  'yearly'  , ''       , ''
!
   ln_abswind      = .true.  ! use absolute wind velocity ( no surface current taken into account)
   ln_abswind_ice  = .true.  ! same as above for the ice
/
```

```
&namsbc_core   !   namsbc_core  CORE bulk formulae   *** ORCA12.L46-MJM88 ***
!-----------------------------------------------------------------------
!             !  file name         ! frequency (hours) ! variable  ! time interp. !  clim  ! 'yearly'/ ! weights  ! rotation !
!             !                    !  (if <0  months)  !   name    !   (logical)  !  (T/F) ! 'monthly' ! filename ! pairing  !
!
   sn_wndi =    'drowned_u10_DFS4.4'   ,     6        ,  'u10'     ,    .true.      , .false. ,  'yearly'  ,  'wght_bicub_ERA40_ORCA12.nc'  , 'U1'
   sn_wndj =    'drowned_v10_DFS4.4'   ,     6        ,  'v10'     ,    .true.      , .false. ,  'yearly'  ,  'wght_bicub_ERA40_ORCA12.nc'  , 'V1'
   sn_qsr  =    'drowned_radsw_DFS4.4' ,    24        ,  'radsw'   ,    .false.     , .false. ,  'yearly'  ,  'wght_bilin_NCAR_ORCA12.nc' ,  ''
   sn_qlw  =    'drowned_radlw_DFS4.4' ,    24        ,  'radlw'   ,    .false.     , .false. ,  'yearly'  ,  'wght_bilin_NCAR_ORCA12.nc' ,  ''
   sn_tair =    'drowned_t2_DFS4.4'    ,     6        ,  't2'      ,    .true.      , .false. ,  'yearly'  ,  'wght_bilin_ERA40_ORCA12.nc' ,  ''
   sn_humi =    'drowned_q2_DFS4.4'    ,     6        ,  'q2'      ,    .true.      , .false. ,  'yearly'  ,  'wght_bilin_ERA40_ORCA12.nc' ,  ''
   sn_prec =    'drowned_precip_DFS4.4' ,   -1        ,  'precip'  ,    .true.      , .false. ,  'yearly'  ,  'wght_bilin_NCAR_ORCA12.nc' ,  ''
   sn_snow =    'drowned_snow_DFS4.4'  ,    -1        ,  'snow'    ,    .true.      , .false. ,  'yearly'  ,  'wght_bilin_NCAR_ORCA12.nc' ,  ''
   sn_tdif =     'taudif'              ,    24        ,  'taudif'  ,    .true.      , .false. ,  'yearly'  ,  ''                  ,   ''

!
   cn_dir      = './'      !  root directory for the location of the bulk files
   ln_2m       = .true.    !  air temperature and humidity referenced at 2m (T) instead 10m (F)
   ln_taudif   = .false.   !  HF tau contribution: use "mean of stress module - module of the mean stress" data
   rn_pfac     = 1.00      !  multiplicative factor for precipitation (total & snow)

   ln_kata     = .false.    ! katabatic wind enhancement
!             !  file name                   ! frequency (hours) ! variable  ! time interp. !  clim  ! 'yearly'/ ! weights  ! rotation !
!             !                              !  (if <0  months)  !   name    !   (logical)  !  (T/F) ! 'monthly' ! filename ! pairing  !
   sn_kati     =     'katamask'     ,      -1           , 'katamaskx',    .false.     , .true.  ,  'yearly'  , ''       , ''
   sn_katj     =     'katamask'     ,      -1           , 'katamasky',    .false.     , .true.  ,  'yearly'  , ''       , ''
!
   ln_abswind      = .true.  ! use absolute wind velocity ( no surface current taken into account)
   ln_abswind_ice  = .true.  ! same as above for the ice
/
```

3.3 Light penetration algorithm according to ocean color

The penetration of the solar flux was parameterized using the available RGB method in the code. This mean that the ocean surface color (interpreted as chlorophyll concentration) is taken into account, and the visible light is splitted into three wavebands: blue (400-500nm), green (500-600nm), red (600-700nm), with their own penetration law (Lengaigne, 2007)[16].
Ocean color data is a SeaWIFS monthly climatology, provided by Sebastien Masson in the file *chlaseawifs_c1m-99-05_smooth_ORCA_R12.nc*
Recent study done at Mercator showed that using this parameterization, a warm surface bias appears, as high as 3°C in the tropical regions. This is because in this parameterization, the chlorophyll concerns only the first level of the model, hence giving a too strong light absorption in this level. A fix is being produced, using the more standard 2-wavebands absorption law (Jerlov's law), modulated in time by the ocean color product. This fix will be used in the next simulations. Reference a mettre vers un talk mercator a drakkar ??

```
&namtra_qsr    !   penetrative solar radiation
!-----------------------------------------------------------------------
!              !  file name                  ! frequency (hours)! variable ! time interp. !  clim  ! 'yearly'/ ! weights  ! rota
!              !                             !  (if <0  months) !   name   !   (logical)  !  (T/F) ! 'monthly' ! filename ! pair
   sn_chl      = 'chlaseawifs_c1m-99-05_smooth_ORCA_R12'  , -1  , 'CHLA'   ,   .true.     , .true. , 'yearly'  , ''       , ''

   cn_dir      = './'      !  root directory for the location of the runoff files
   ln_traqsr   = .true.    !  Light penetration (T) or not (F)
   ln_qsr_rgb  = .true.    !  RGB (Red-Green-Blue) light penetration
   ln_qsr_2bd  = .false.   !  2 bands              light penetration
   ln_qsr_bio  = .false.   !  bio-model light penetration
   nn_chldta   =      1    !  RGB : Chl data (=1) or cst value (=0)
   rn_abs      =   0.58    !  RGB & 2 bands: fraction of light (rn_si1)
   rn_si0      =   0.35    !  RGB & 2 bands: shortess depth of extinction
   rn_si1      =   23.0    !  2 bands: longest depth of extinction
/
```

3.4 Diurnal Cycle on solar fluxes

The parametrization of the diurnal cycle on the solar flux is used in this simulation (ln_dm2dc=.true.), although the 46-level vertical discretization gives surface layers of about 6 meters. We did this choice to be coherent with the corresponding twin ORCA025 simulation which has 75-level vertical grid (hence about 1m resolution near the surface).

3.5 River Run-off

The coastal and river run-off data are read in the file *runoff_obtaz_rhone_1m_ORCA12_20102008_iceberg.nc*, already used in ORCA12.L46-MAL101 simulation, and whose making-of was related in ORCA12.L46-MAL101 report (Lecointre, 2012) [15]. It is mainly based on the Dai and Trenberth (2002)[5] monthly climatology for 119 rivers and coastal runoff estimates. This version of the file also includes an estimate of the Antarctic runoff due to iceberg calving (Silva et al., 2006 [22]).

For the construction of this file, the original antarctic coastal runoff (available in the previous version of the runoff file), has been reduced by the monthly estimate of the Silva et al. (2006), while this latter estimate has been added with the pattern given in [22]. With this modification, the total runoff is kept unchanged compared to previously used files. In table 4,

the different estimates of annual mean runoff (in Sv) is given, for the Global Ocean and for the Southern Ocean only (south of 60 °S). The mask defining the grid points where runoff is applied is shown on figure 8. On those points, the SSS restoring is inhibited.

At river mouth, the vertical mixing coefficient between layers 1 and 2 is increased by $2.3 m^2/s$. Run-off are just considered as additional precipitations, spanned over the river mouth, no temperature nor salinity information is used.

Moy annuelle (Sv)	**initial**	**iceberg**	**final**
Global	1.3147	0.0206	1.3201
South of 60S	0.0828	0.0152	0.0828

Table 4: Global and South of 60S runoff in initial runoff file, in only-iceberg runoff, and in final runoff file used in MAL101, GJM02 and MJM88 simulations

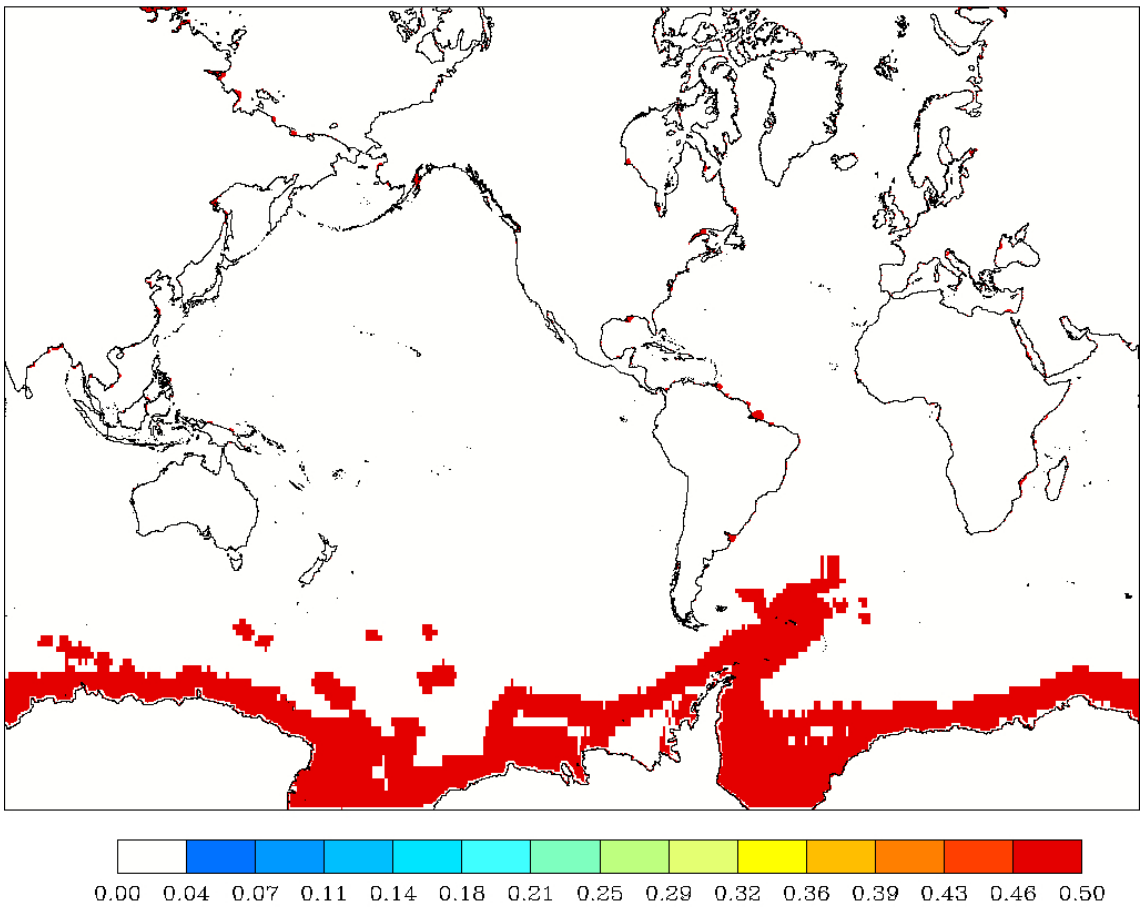

Figure 8: Runoff mask showing the imprint of the icebergs. All along the coasts, a coastal runoff is applied, on 1 grid point, and is not well represented on this global scale map.

```
&namsbc_rnf    !   runoffs namelist surface boundary condition
!-----------------------------------------------------------------------
!             !  file name           ! frequency (hours) ! variable  ! time interp. !  clim  ! 'yearly'/ ! weights  ! rotation
!             !                      !  (if <0  months)  !   name    !   (logical)  !  (T/F) ! 'monthly' ! filename ! pairing
   sn_rnf      = 'runoff_MAL101'    , -1 , 'sorunoff', .true.  , .true. , 'yearly'  , ''       , ''
   sn_cnf      = 'runoff_MAL101'    ,  0 , 'socoefr',  .false. , .true. , 'yearly'  , ''       , ''
   sn_s_rnf    = ' '             ,        24         , 'rosaline',   .true.     , .true. , 'yearly'  , ''       , ''
   sn_t_rnf    = ' '             ,        24         , 'rotemper',   .true.     , .true. , 'yearly'  , ''       , ''
   sn_dep_rnf  = ' '             ,         0         , 'rodepth' ,   .false.    , .true. , 'yearly'  , ''       , ''

   cn_dir       = './'      !  root directory for the location of the runoff files
   ln_rnf_emp   = .false.   !  runoffs included into precipitation field (T) or into a file (F)
   ln_rnf_mouth = .true.    !  specific treatment at rivers mouths
   rn_hrnf      =  10.e0    !  depth over which enhanced vertical mixing is used
   rn_avt_rnf   =   2.e-3   !  value of the additional vertical mixing coef. [m2/s]
   rn_rfact     =   1.e0    !  multiplicative factor for runoff
   ln_rnf_depth = .false.   !  read in depth information for runoff
   ln_rnf_tem   = .false.   !  read in temperature information for runoff
   ln_rnf_sal   = .false.   !  read in salinity information for runoff

! ************************************************************************************
! ***** runoff_MAL101 is a link to runoff_obtaz_rhone_1m_ORCA12_20102008_iceberg.nc ****!
! ************************************************************************************
/
```

3.6 SSS restoring strategy

Sea Surface Salinity restoring is necessary to avoid a drift of the model salinity. Among the many reasons that may produce this drift, is is worth to mention (i) the inacuracy of fresh water fluxes in the forcing function, (ii) the lack of feed-back from the atmosphere in forced mode. However, the available global SSS data (up to now) are at best monthly climatology such as the World Ocean Atlas (Levitus, 2009). These climatology are by construction very smooth. Therefore, the restoring term, which is proportional to the model-climatology mismatch ($SSS_{mod} - SSS_{clim}$) can be very strong at the meso-scale. On the other hand, the low spatial resolution of climatological data, impeeds the correct representation of boundary currents (e.g. WBC), and their imprint on SSS (and SST by the way). For these reasons, a non standard method has been implemented in the recent DRAKKAR runs:

– compute the mismatch SSS estimate from spatially filtered model SSS: $\overline{SSS_{mod}} - SSS_{clim}$. $\overline{SSS_{mod}}$ is computed iterating a shapiro filter on the model SSS. The number of iteration of the filter is specified in the namelist ($nn\_shap\_iter = 300$). The choice of a shapiro filter was mainly done for computational reasons. Any filter with larger span is problematic in parallel environment.

– avoid restoring near the continental coasts, using a predefined file (figure 9) giving the distance to the continents for a given ocean point. Islands are not taken into account in the file. The lenght scale for the restoring fading out is $rn\_dist = 150km$.

– using a threshold ($4mm/day$) for the restoring term. This is a standard feature of NEMO, using namelist parameter rn_sssr_bnd

The piston veolocity used for this SSS restoring is $166.667mm/day$ corresponding to a time scale of 60 days for the upper 10 meters of the ocean. As in other DRAKKAR simulations, the restoring term (thought as a correction to E-P term) is also taken into account in the SSH evolution equation.

```
&namsbc_ssr    !   surface boundary condition : sea surface restoring
!-----------------------------------------------------------------------
!             !     file name      ! frequency (hours) ! variable   ! time interpol. !  clim   ! 'yearly' / ! weights  ! rotati
```

```
!             !                    !  (if <0  months)  !   name     !    (logical)   !  (T/F)  ! 'monthly'  ! filename ! pairi
   sn_sst     =    ' '              ,        24         , 'sst'      ,     .false.    , .false. ,  'yearly'   , ''       , ''
   sn_sss     =    'Levitus_p2.1_1m_01_12_sss_correc_mms025_ORCA_R12' ,        -1         ,  'vosaline' ,  .true.    , .true.
!!
   cn_dir     = './'      !  root directory for the location of the runoff files
   nn_sstr    =     0     !  add a retroaction term in the surface heat       flux (=1) or not (=0)
   nn_sssr    =     2     !  add a damping     term in the surface freshwater flux (=2)
                          !  or to SSS only (=1) or no damping term (=0)
   rn_dqdt    =   -40.    !  magnitude of the retroaction on temperature   [W/m2/K]
   rn_deds    =  -166.667 !  magnitude of the damping on salinity   [mm/day]
   ln_sssr_bnd =   .true.  !  flag to bound erp term (associated with nn_sssr=2)
   rn_sssr_bnd =   4.e0    !  ABS(Max/Min) value of the damping erp term [mm/day]

   ln_sssr_flt = .true.    ! use filtering of SSS model for sss restoring
   nn_shap_iter   =  300   ! number of iteration of the shapiro filter
   ln_sssr_msk = .true.    ! use a mask near the coast
!             !  file name  ! frequency (hours) ! variable  ! time interp. !  clim  ! 'yearly'/ ! weights  ! rotation !
!             !             !  (if <0  months)  !   name    !   (logical)  !  (T/F) ! 'monthly' ! filename ! pairing  !
   sn_coast    = 'dist_coast_modif_RD_closed_seas_corrected_nodepth_R12' ,         0         , 'Tcoast'  , .false.      , .true
   rn_dist    =  150.      ! distance to the coast
/
```

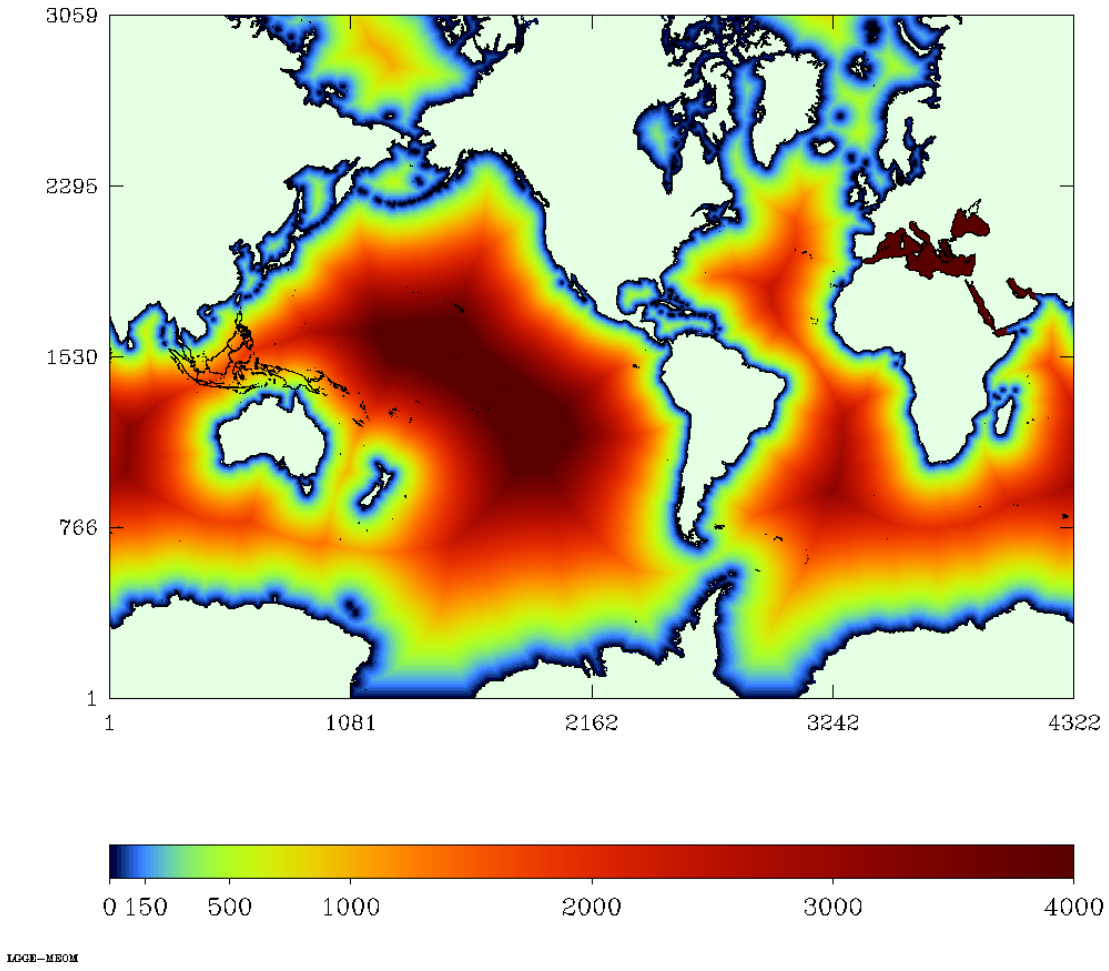

Figure 9: Distance to the continental coast, used for fading out SSS restoring in a 150 km wide coastal stripe.

3.7 LIM2 ice model

3.7.1 EVP and VP rheology

For ORCA12.L46-GJM02, EVP rheology was used for the first 11 years (0001 to 0011). A persistant problem of spurious polynia opening in the Weddell sea appears, and among all the tests performed in order to get rid of it, the change from EVP to VP rheology was done. Unfortunatly this did not fix the polynia problem (it was fixed by light TS restoring in the upper Weddell Sea), but we keep it for the rest of the run (0012 to 0085). For coherency, interannual run ORCA12.L46-MJM88 also used VP rheology with same parameters.
Although the change from EVP to VP was not foreseen at the begining of the run, large changes in the Arctic Ocean, and particularly in the ice thickness of the Beaufort Sea. More will be said in the validation section. Therefore, it is worth to be noted than the ice model is still an issue in ORCA12 runs, and that a clear assessment of the ice control parameters is needed for future runs.

3.7.2 Thermodynamics

The standard LIM2 thermodynamics is used. The only change with respect to the standard code is the use of cloud cover files (synoptic) instead of a standard constant value for nebulosity. It has an impact on the net shortwave radiation which is not absorbed in the thin surface layer and penetrates inside the ice cover. The sensitivity of the ice solution to this change is not assessed yet. Unfortunatly, this change was done only for the climatological run (GJM02) and not for the interannual one (MJM88).

```
&namicedyn     !   ice dynamic
!-----------------------------------------------------------------------
   epsd        =   1.0e-20 !  tolerance parameter
   alpha       =   0.5     !  coefficient for semi-implicit coriolis
   dm          =   0.0e+03 !  diffusion constant for dynamics
   nbiter      =   1       !  number of sub-time steps for relaxation
   nbitdr      = 550       !  maximum number of iterations for relaxation
   om          =   0.5     !  relaxation constant
   resl        =   5.0e-05 !  maximum value for the residual of relaxation
   cw          =   5.0e-03 !  drag coefficient for oceanic stress
   angvg       =   0.0     !  turning angle for oceanic stress
   pstar       =   1.0e+04 !  1st bulk-rheology parameter
   c_rhg       =  20.0     !  2nd bulk-rhelogy parameter
   etamn       =   0.0e+07 !  minimun value for viscosity
   creepl      =  20.0e-09 !  creep limit
   ecc         =   2.0     !  eccentricity of the elliptical yield curve
   ahi0        = 200.e0     !  horizontal eddy diffusivity coefficient for sea-ice [m2/s]
   nevp        = 120       !  number of iterations for subcycling
   telast      = 640       !  timescale for elastic waves
   alphaevp    = 1.0       !  coefficient for the solution of int. stresses
/
&namicethd     !   ice thermodynamic
!-----------------------------------------------------------------------
   hmelt       = -0.15     !  maximum melting at the bottom
   hiccrit     = 0.6 , 0.3 !  ice thickness for lateral accretion in the Northern (Southern) Hemisphere
   !                       !  (caution 1.0, 1.0 best value to be used!!! (gilles G.))
   hicmin      = 0.2       !  ice thickness corr. to max. energy stored in brine pocket
   hiclim      = 0.05      !  minimum ice thickness
   amax        = 0.999     !  maximum lead fraction
   swiqst      = 1.        !  energy stored in brine pocket (=1) or not (=0)
   sbeta       = 1.        !  numerical caracteritic of the scheme for diffusion in ice
                           !       Cranck-Nicholson (=0.5), implicit (=1), explicit (=0)
   parlat      = 0.0       !  percentage of energy used for lateral ablation
   hakspl      = 0.5       !  slope of distr. for Hakkinen-Mellor's lateral melting
   hibspl      = 0.5       !  slope of distribution for Hibler's lateral melting
   exld        = 2.0       !  exponent for leads-closure rate
   hakdif      = 1.0       !  coefficient for diffusions of ice and snow
   thth        = 0.2       !  threshold thickness for comp. of eq. thermal conductivity
   hnzst       = 0.1       !  thickness of the surf. layer in temp. computation
   parsub      = 1.0       !  switch for snow sublimation or not
   alphs       = 1.0       !  coefficient for snow density when snow ice formation
/
```

4 Run production

4.1 Overview

Run ORCA12.L46-GJM02 was integrated for 85 years, with DFS4.4 climatological forcing, years 0001 to 0085. Overall, with the setting up of the model on ada at IDRIS, the cost for this simulation was about 5 millions CPU hours. The data set produced during this run occupy about 100 Tb on the gaya storage machine at IDRIS.

Run ORCA12.L46-MJM88 was run for 55 years, with DFS4.4 inter-annual forcing, years 1958 to 2012. This run included CFC^{11} passive tracer simulation. Overall, the cost of this run on jade at CINES amounted to about 3 millions CPU hours. The data set produced during this run occupy 110 Tb on the CINES storage machine.

4.2 Integration and computing performance

4.2.1 Domain decomposition

Run ORCA12.L46-GJM02 was performed at IDRIS HPC center, on the brand new 'ada' computer (IBM X3750, see IDRIS website for details – http://www.idris.fr –), during the 'Grands Challenges 2012'. During the 'Grands Challenges' neither limits on the number of cores, nor on the cpu time were fixed. After some quick scalability tests (figure 10), a domain decomposition on 3584 cores (112 nodes of 16 cores) was choosen (figure 11). It is worth to be noted than in normal production mode, it is not possible to use more than 2048 cores (64 nodes), which by the way is under-optimal for ORCA12 configurations.

Run ORCA12.L46-MJM88 was performed at CINES HPC center on 'jade' (SGI Altix ICE 8200 cluster). A domain decomposion on 3056 cores (382 nodes of 8 cores). Although there are no limits in the number of requested cores in the CINES batch system (–except the hardware limit–), this choice is a trade-off between computing efficiency and queue time. No dedicated scalability tests were performed on 'jade' for MJM88 as extensive scalability analysis was already performed for previous configurations than ran on 'jade' (Lecointre et al., 2011[14], Lecointre, 2012[13]). However, one year of GJM02 was repeated on jade, on 3584 cores and the corresponding perfs (in step/mn) is plotted on figure 10 as a green dot. It can be seen that the thin nodes (8 cores per node) of jade are more efficient to run ORCA12 than the fat nodes (32 cores per node) of ada. This poor result for ada should be modulated by the fact that no tests on the core-binding have been done on ada, while on jade, the core binding ('by node') prooved to increase the perfs by almost 40%. (Default core binding on ada is binding 'by core'). Tests regarding this issue are to be done before 2014 computational campaign.

It is worth to note that domain decomposition optimization is made easier by the use of the *MPP_PREP* tool, and in particular by the DRAKKAR update of this tool, available in DCM. With *mpp_optimize*, any possible domain decomposition (in term of *jpni*, *jpnj*, *jpnij*) corresponding to a bathymetric file is given in the output file. Then a usefull script (*screen.ksh*) us used to perform data screening of the results, to give all possible choice for a fixed number of cores. The result of the command *screen.ksh* 3584 is shown below:

```
Searching for 3584 sea processors in processor.layout.orca12_bathy_v3.3_bis ....
jpni  jpnj   jpi   jpj  jpi x jpj  proc  elim   sup
   2  1792  2162     4       8648  3584     0  2.34433
   8   531   542     8       4336  3584   664  1.17542
  13   347   335    11       3685  3584   927  0.99894
```

24	200	182	18	3276	3584	1216	0.88807	
25	194	175	18	3150	3584	1266	0.85391	
32	154	137	22	3014	3584	1344	0.81705	
58	87	77	38	2926	3584	1462	0.79319	***
222	22	22	141	3102	3584	1300	0.84090	
315	15	16	206	3296	3584	1141	0.89349	
452	10	12	308	3696	3584	936	1.00193	
677	6	9	512	4608	3584	478	1.24916	
1792	2	5	1531	7655	3584	0	2.07515	
3584	1	4	3059	12236	3584	0	3.31698	

Last column give the ratio between the number of computed grid point and the total number of grid points in the domain. Optimal decomposition corresponds to the lowest ratio. In the example, for 3584 cores the optimal decomposition is $jpni = 58, jpnj = 87$.

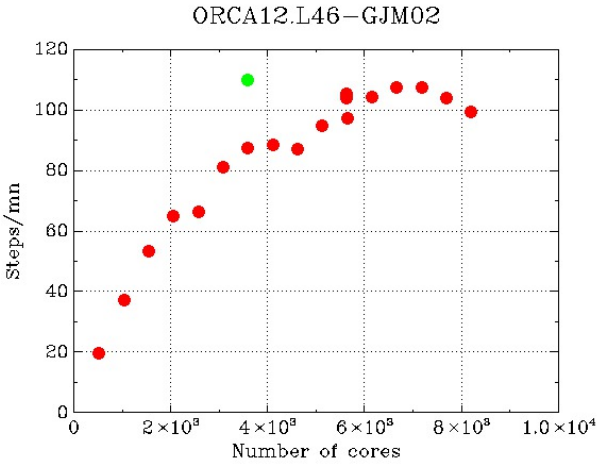

Figure 10: Scalability tests: number of step/mn vs number of core. Red dots corresponds to ada performances. The single green dot correspond to one experiment repeated on jade.

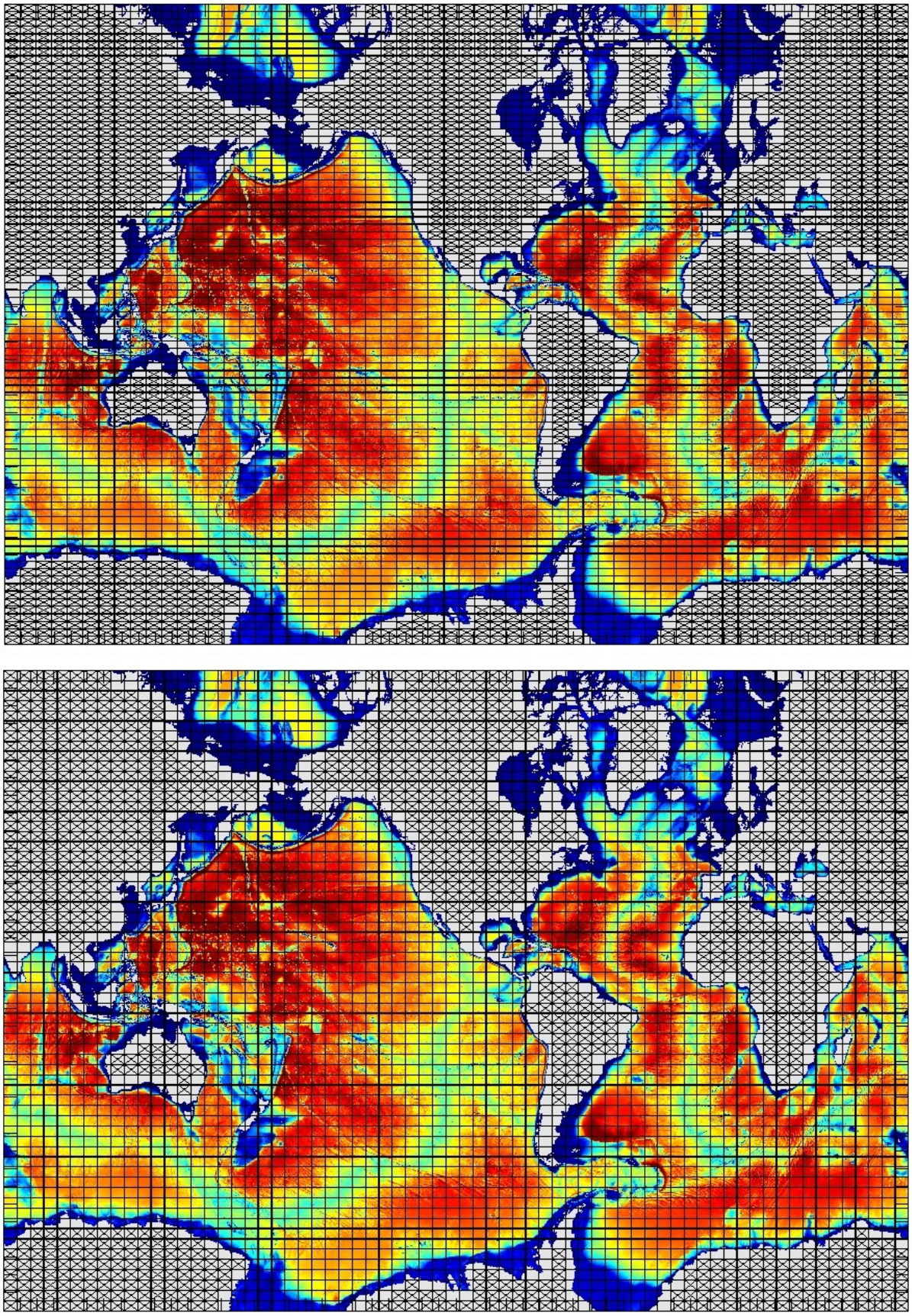

Figure 11: Domain decomposition for GJM02 (top) and MJM88 (bottom). Domains marked with x have land-only points and are not used in the computation.

```
&nammpp        !   Massively Parallel Processing                      ("key_mpp_mpi)
!-----------------------------------------------------------------------
```

```
   cn_mpi_send =  'I'      !  mpi send/recieve type   ='S', 'B', or 'I' for standard send,
                           !  buffer blocking send or immediate non-blocking sends, resp.
   nn_buffer   =   0       !  size in bytes of exported buffer ('B' case), 0 no exportation
   ln_nnogather=  .true.   !  activate code to avoid mpi_allgather use at the northfold
!
! *** ORCA12.L46-GJM02 ***
   jpni        =  58    !  jpni   number of processors following i (set automatically if < 1)
   jpnj        =  87    !  jpnj   number of processors following j (set automatically if < 1)
   jpnij       =  3584  !  jpnij  number of local domains (set automatically if < 1)

! *** ORCA12.L46-MJM88 ***
   jpni        =  68    !  jpni   number of processors following i (set automatically if < 1)
   jpnj        =  63    !  jpnj   number of processors following j (set automatically if < 1)
   jpnij       =  3056  !  jpnij  number of local domains (set automatically if < 1)
/
```

4.2.2 Choice of elliptic solver

For the computation of surface pressure gradient, in the case of filtered linear free surface (this case with key_dynspg_flt defined), an elliptic solver is used. Two options are offered in NEMO : either a preconditioned conjugate gradient solver (PCG) or a successive over relaxation solver (SOR). There were speculations concerning SOR solver efficiency for large mesh (as ORCA12). Lecointre (2012)[12] showed that computing performance doesn't increase when using SOR rather than PCG solver, even when tuning *rn_sor* value. The tuning of the *rn_sor* value is quite tedious and a very small departure from the optimal value may completely degrade the performances of the code. According to these results, for safety reasons, PCG solver was used, as in all the DRAKKAR configurations run in Grenoble so far.

```
&namsol        !   elliptic solver / island / free surface
!-----------------------------------------------------------------------
   nn_solv     =      1    !  elliptic solver: =1 preconditioned conjugate gradient (pcg)
                           !                   =2 successive-over-relaxation (sor)
   nn_sol_arp  =      0    !  absolute/relative (0/1) precision convergence test
   rn_eps      =  1.e-6    !  absolute precision of the solver
   nn_nmin     =    390    !  minimum of iterations for the SOR solver
   nn_nmax     =  15000    !  maximum of iterations for the SOR solver
   nn_nmod     =     10    !  frequency of test for the SOR solver
   rn_resmax   =  1.e-10   !  absolute precision for the SOR solver
   rn_sor      =  1.973    !  optimal coefficient for SOR solver (to be adjusted with the domain)
/
```

4.2.3 North pole folding condition

Since release 3.4 of NEMO, the north pole folding condition can be performed avoiding costly mpi_gather operations (Donners, 2011), which leads to a significant increase in model performances for ORCA12, in particular when combined with optimal task placement (core binding by node) (details in Lecointre, 2011[13]). This new algorithm for north fold condition is now used as standard for the DRAKKAR global runs (*ln_nnogather* = *.true.*). Recent extra optimization on this same north pole folding condition, (work of I. Epicoco, INGV) gave up to 20% improvements on some architecture. This will be tested on the machines DRAKKAR.fr is running, before next campaign.

4.3 Model output strategy

For the climatological run ORCA12.L46-GJM02, the monthly mean of all fields (3D + 2D) are saved as a basis. For the last 14 years, the output frequency is reduced to 5 days. In addition, 2D surface fields (SSH, SST, SSS, SSU and SSV) are saved as 5 day average, for the whole period of the run (0001–0085). For the last 14 years, the same surface fields are saved as daily averages.

For the interannual run ORCA12.L46-MJM88, 5 days average of 3D +2D fields are saved for the whole period (1958–2012). A secondary data set for surface fields (SST, SSS, SSH, SSU and SSV) is saved at the same 5d frecuency.

Then for both runs, monthly and annual averages are stored in the respective -MEAN directory. A 10 year climatology is also computed for validation of the model mean state.

4.4 Journal of the run

For both runs, in order to achieve the first geostrophic adjustment, the time-step has been slowly increased from 72 seconds to 480 seconds during the first month of the run. Then the time step of 480 seconds remains constant till the end of the run. The first year of both runs was done following the following road-map :

```
!  Run   Day      Steps       nn_write      rn_rdt(min/max)
!  1     1-5      1-6000         6000            72
!  2     6-15     6001-12000     3000            144
!  3     16-30    12001-15600    1200            360
!  4     31-365   15601-75900     900            480
!  5     366-730  75901-141600    900            480
```

As already mentioned, ORCA12.L46-GJM02 required adjustments during the first 15 years of the run, because a robust spurious polynia appears in the center of the Weddell Sea. A summary of the adjustments is given below. Note that these adjustments were part of tests, conducted with trial and error method and with the pressure of finding quickly a solution to the polynia problem, in the framework of the 'Grands Challenges'. Hopefully, keeping exactly the same fixes for the inter annual run worked and integration of ORCA12.L46-MJM88 was straight forward from the beginning (1958) to the end (2012)!

4.4.1 Adjustments during the 15 first years of ORCA12.L46-GJM02

ice model parameters After 3 years of run, some of the ice parameters were revisited according to P. Mathiot PhD (2009)[18]. It is unclear to infer ice parameters for high resolution sea ice. For instance, fluid mechanics reflex concerning viscosity are likely not to be pertinent for the ice. Additional assessment is required. But, the changes of parameters were inefficient for the elimination of the spurious Weddell Sea polynia. Table 5 summarized the changes.

years	1 – 3	4 – 11	12 – 85
ahi0	50	200	200
pstar	25000	10000	10000
hiccrit	0.6 0.6	0.6 0.3	0.6 0.3
creepl	1.e-9	20.e-9	20.e-9
nevp	120	120	VP
telast	480	640	VP

Table 5: Evolution of ice parameters in namelist_ice during the first year of the GJM02 run.

Weddell Sea TS restoring TS restoring in the central Weddell Sea was very efficient to eliminate spurious polynia there. But the idea was to get rid of this restoring and try to adjust ice model parameters to make the work. Therefore, TS restoring was used to stabilize the situation when changing parameters, then switched off.

TS restoring was turned on from years 5 to 6 then for year 12 to 13, and finally from year 17 to 85. The time scale for this restoring is 1 year.

4.4.2 CFC^{11} in ORCA12.L46-MJM88

For this interannual simulation, starting in 1958, CFC^{11} were added. An initial condition infered from previous ORCA025-G70 run was built for the beginning of 1960. The idea was to let the dynamics of the ocean model forget a little about its initial condition at rest, before advecting passive tracers. At the end of 1997, input data file for CFC was updated to the most recent version ending in 2012, obtained with the help of J. Orr (LSCE). There are small differences between the old and new data set, attributed to changes in data processing. However, at the time of the transition (1997) changes were very small and a simple linear merging was used.

5 Validation

The ORCA12.L46-GJM02 and ORCA12.L46-MJM88 illustrations that are presented in this section are directly taken from the monitoring of the experiments, available on demand on the Drakkar web site (contact bernard.barnier@legi.grenoble-inp.fr). In this particular report, where two companion simulations are presented, and for comparison purposes, most of the plots are presented side by side, when possible.

5.1 Mean state of the ocean

Maps of the time mean of the major ocean variables (temperature, salinity, sea surface height, barotropic transport streamfunction and meridional overturning circulation) are presented in this section. For the climatological experiment, the time mean corresponds to the last 10 years of simulation (0076 to 0085), while for the interannual experiment, it corrresponds to the 8 years-period 2000-2007. This latter choice, was taken for comparison with the first ORCA12 runs, ending in 2007. The mean state of the ocean in the two simulation are very similar, not surprisingly. At least, this is an indication that the adopted forcing strategy worked well and that the variability by itself can be compared safely.

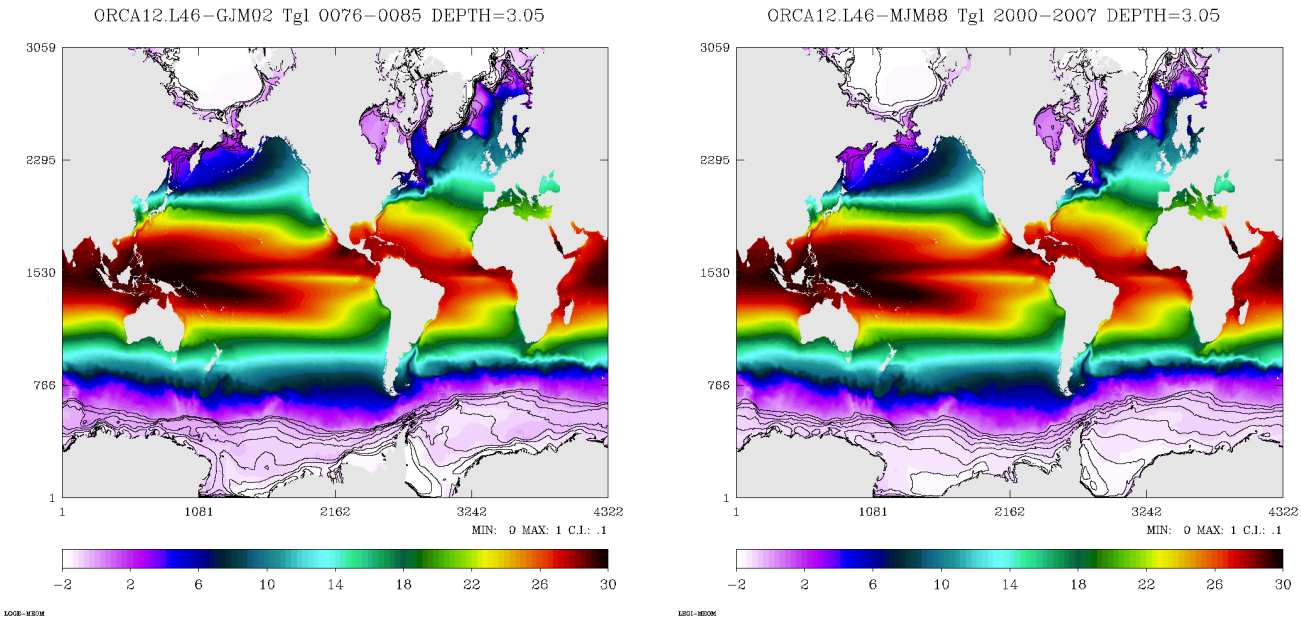

Figure 12: Mean Sea Surface Temperature. Colours indicate the SST in °C, and contour lines indicate the sea ice thickness. Left panel for GJM02, right panel for MJM88.

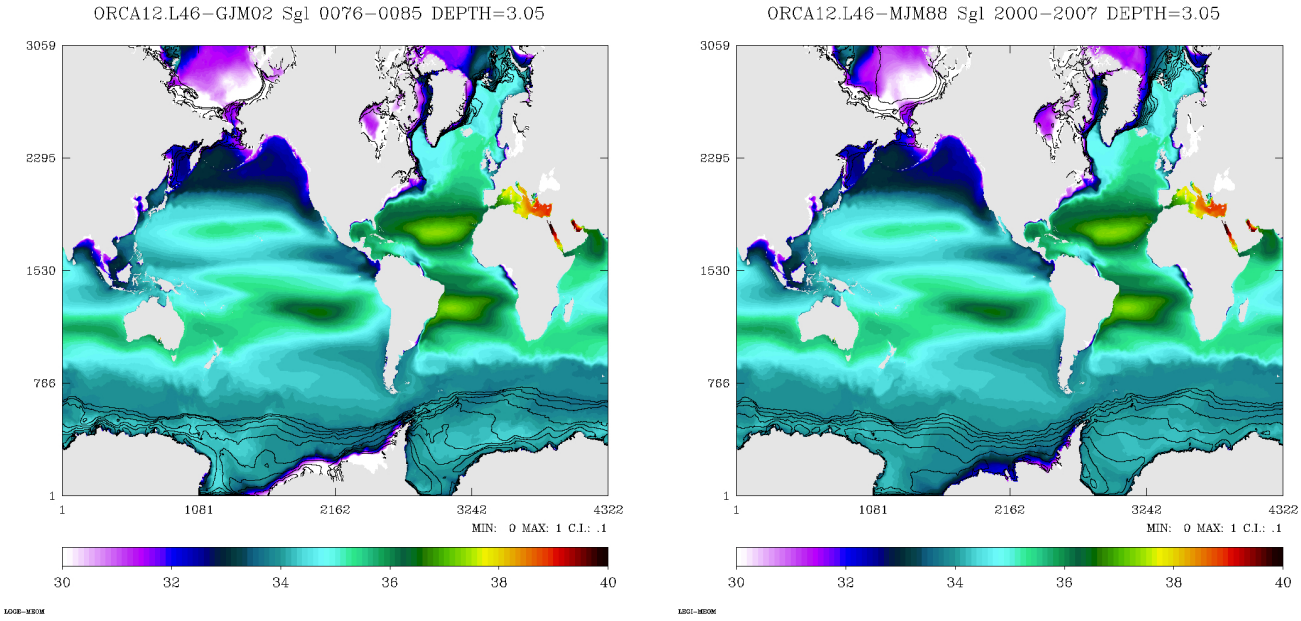

Figure 13: Mean Sea Surface Salinity. Colours indicate the SSS, and contour lines indicate the sea ice thickness. Left panel for GJM02, right panel for MJM88.

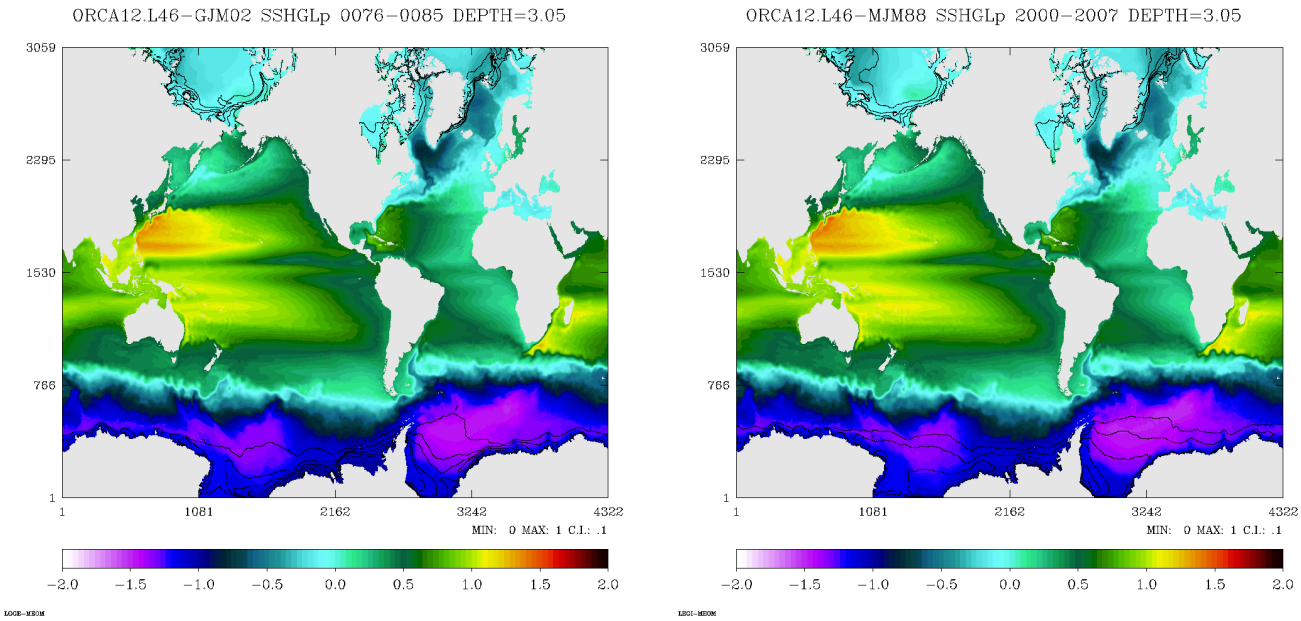

Figure 14: Mean Sea Surface Height. Colours indicate the SSH in meters, and contour lines indicate the sea ice thickness. Left panel for GJM02, right panel for MJM88.

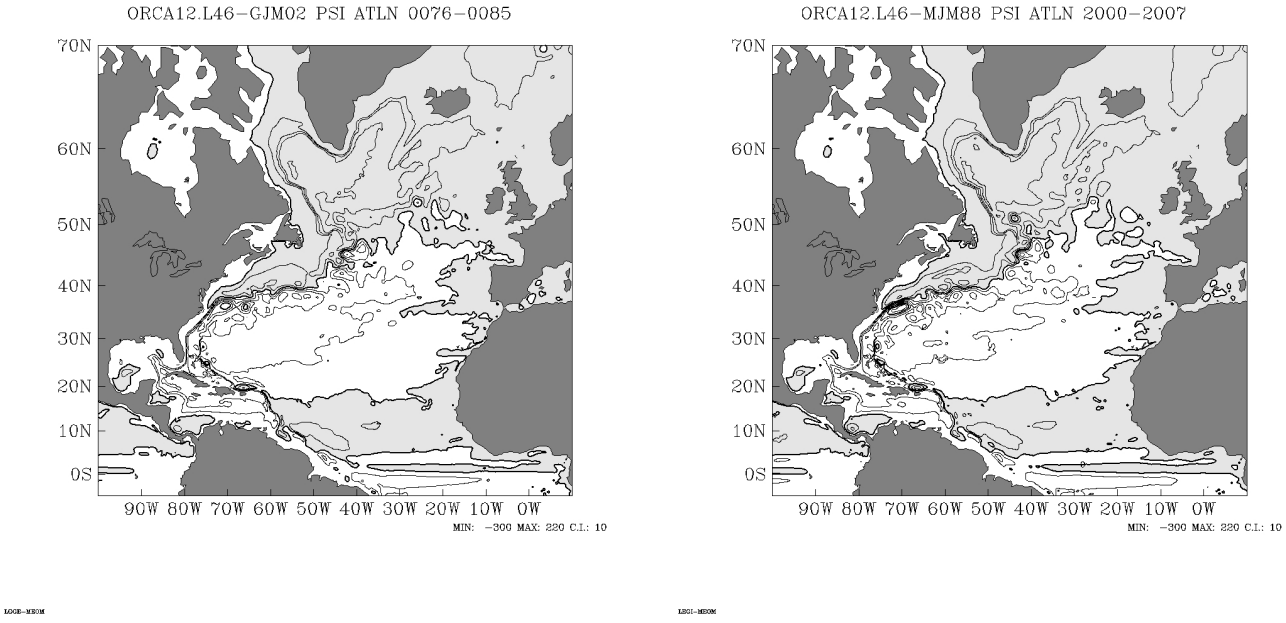

Figure 15: Mean Barotropic Streamfunction. Contours by 10 Sv, negative values are shaded. Left panel for GJM02, right panel for MJM88.

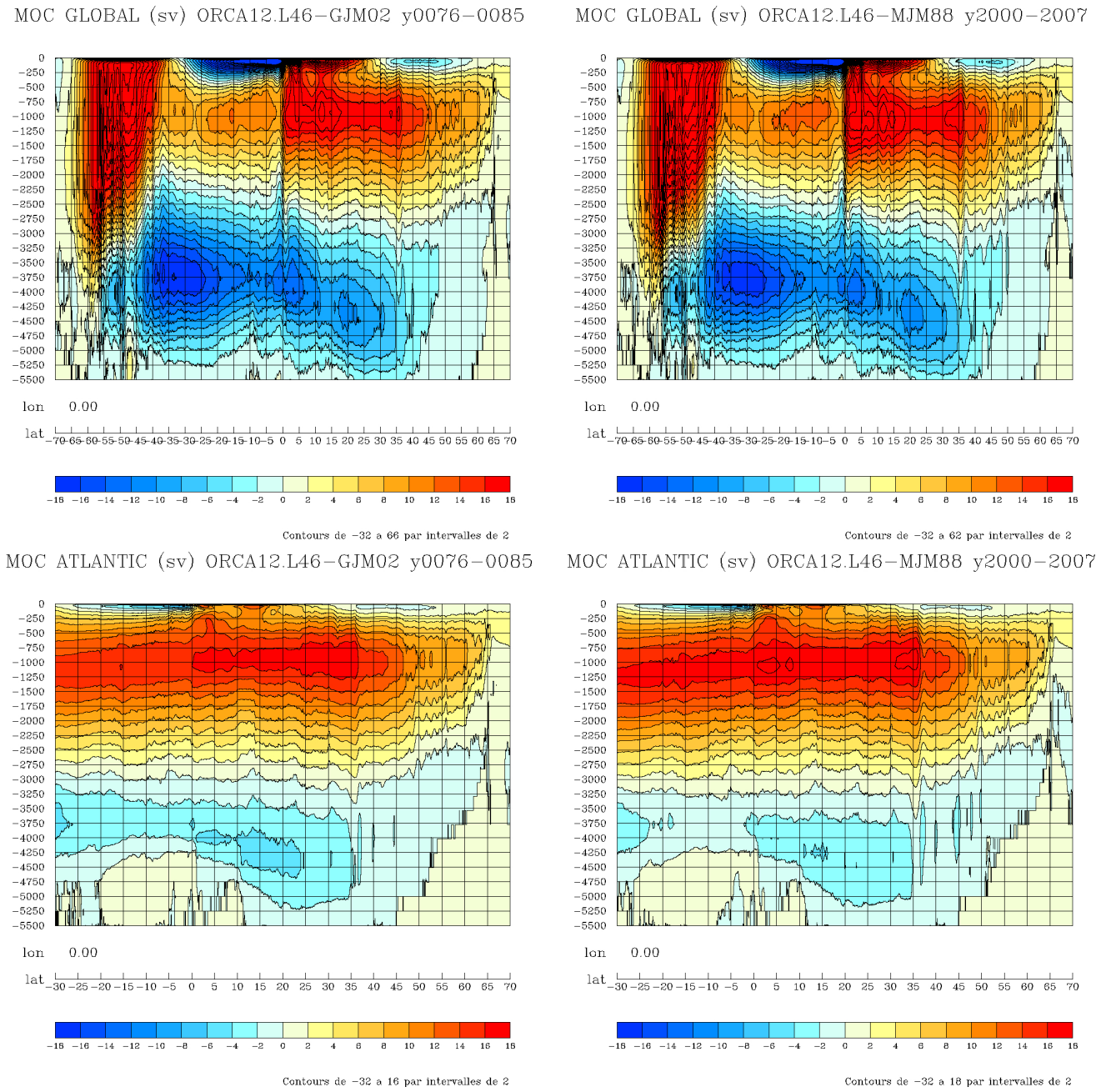

Figure 16: Mean Overturning. Top: Global Ocean, bottom: Atlantic Ocean. Contours by 2 Sv. Left panel for GJM02, right panel for MJM88.

5.2 Temperature and salinity differences with observation climatology (CLASS1-1)

The mean temperature differences with Levitus 1998 climatology at various depths (0m, 100m, 500m) are shown on figures 17 and 18.

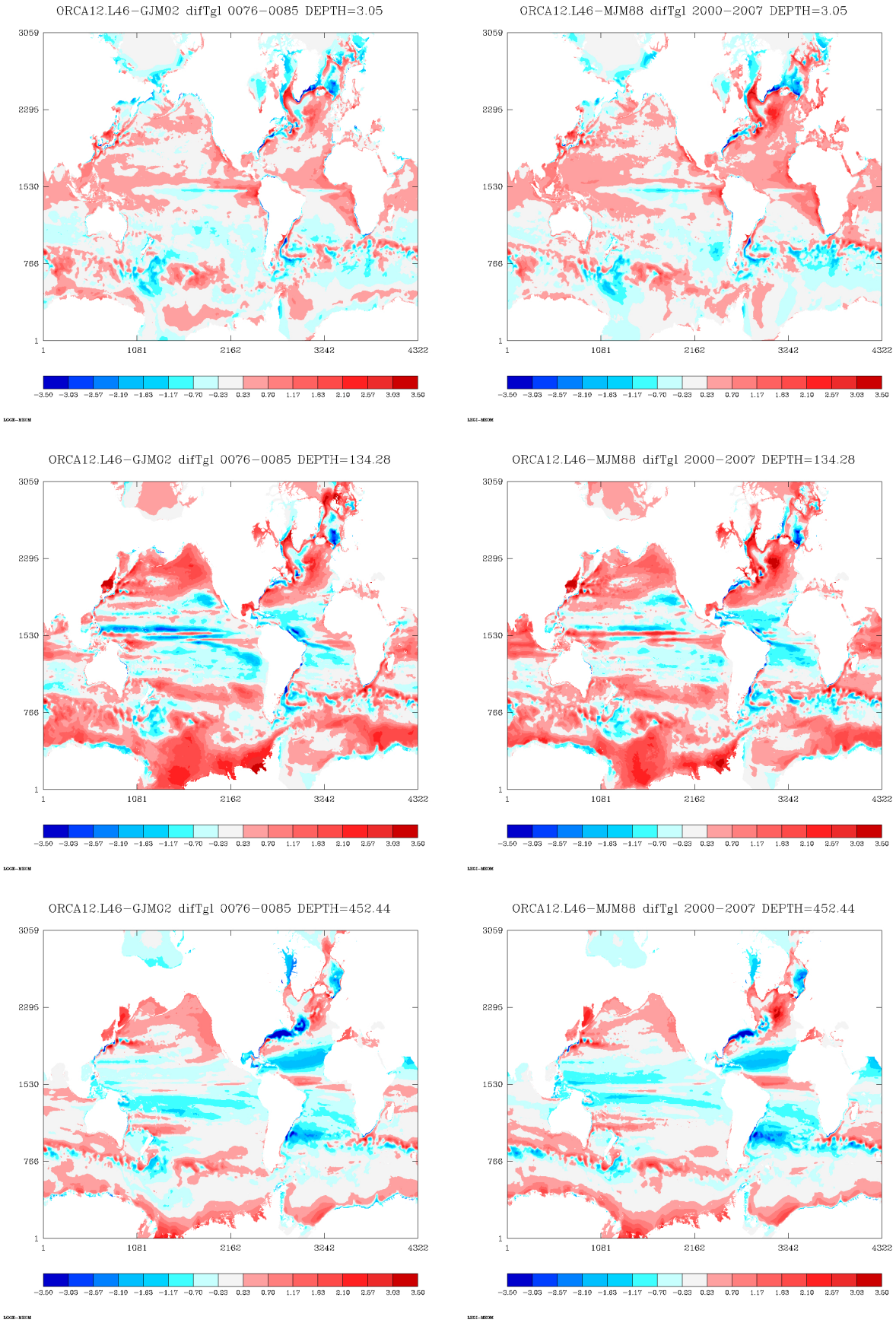

Figure 17: Temperature anomaly with respect to Levitus climatology used for initial conditions, at various depths, for GJM02 on the left, and MJM88 on the right. Positive values (red) indicate a warm bias, whereas negative values (blue) indicate a cold bias.

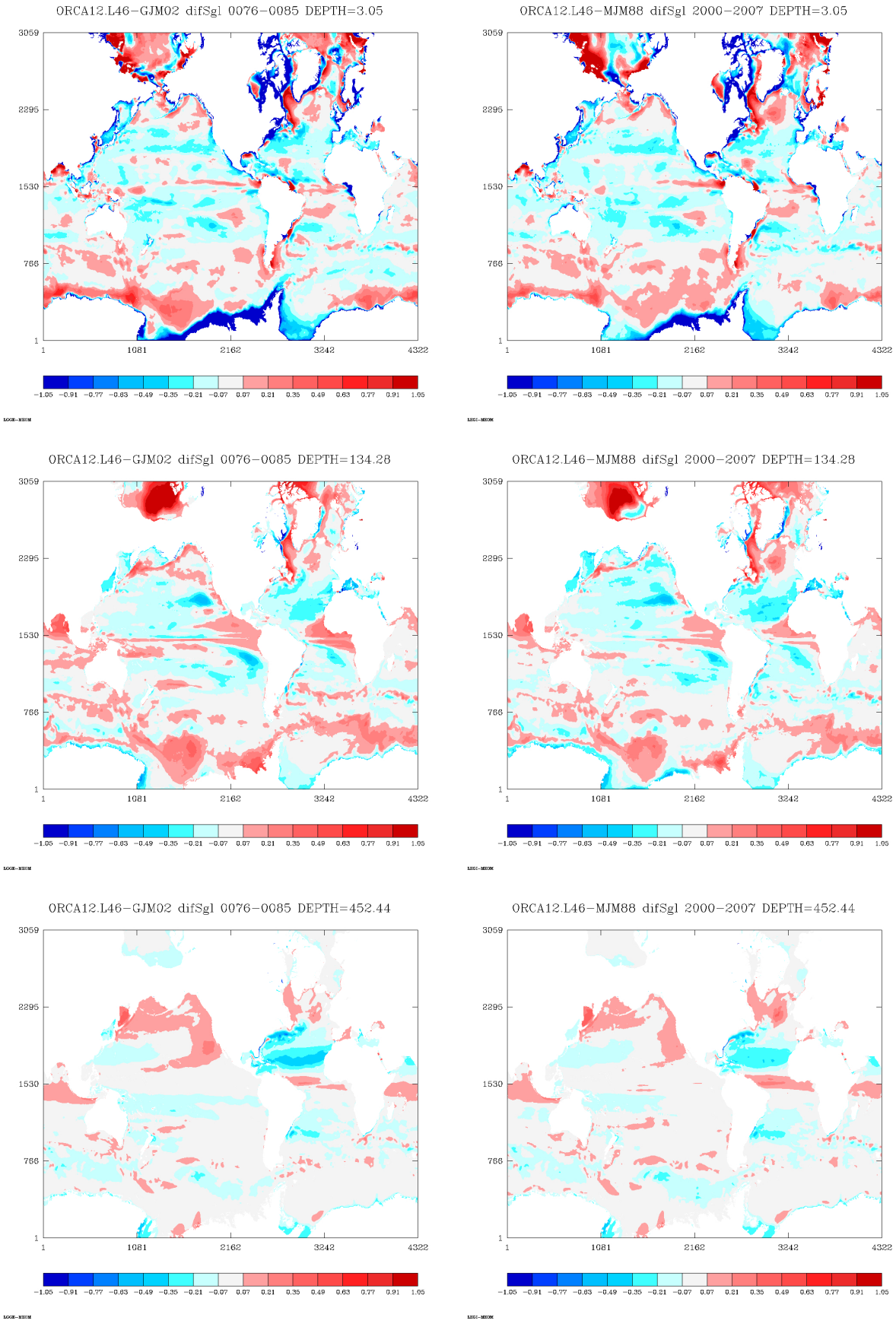

Figure 18: Salinity anomaly with respect to Levitus climatology used for initial conditions, at various depths, for GJM02 on the left, and MJM88 on the right. Positive values (red) indicate a salt bias, whereas negative values (blue) indicate a fresh bias.

5.3 Heat and Freshwater surface fluxes CLASS1-4

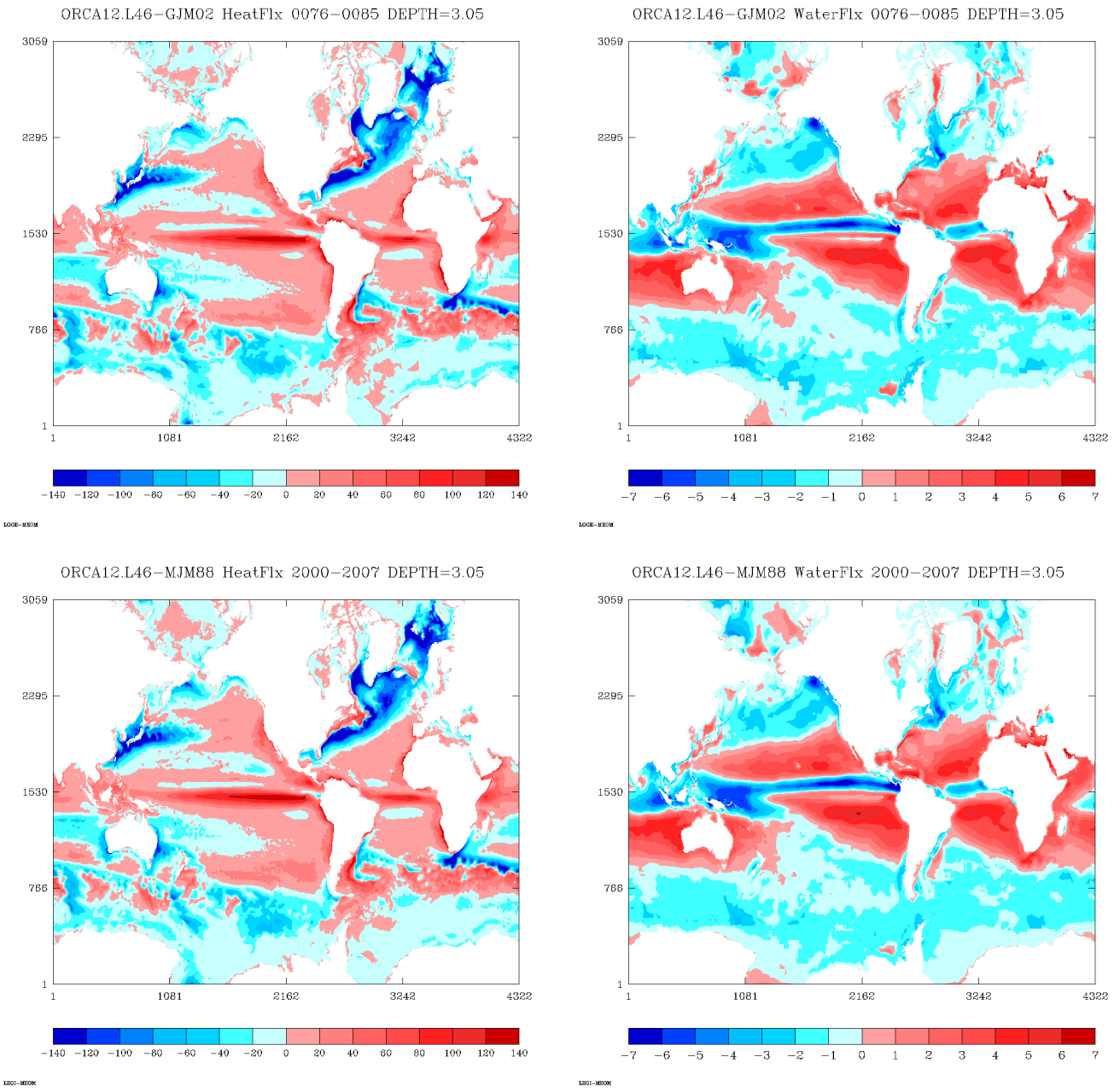

Figure 19: Mean net heat flux in W/m2 (left), and freshwater flux in mm/day (right). Top panel for GJM02, bottom panel for MJM88.

5.4 Sea-Ice CLASS1-3

Mean sea ice concentrations are presented in March and September, for the Arctic (figure 20) and the Antarctic (figure 21). Differences between the climatological and interannual runs are cleary visible, particularly in the Arctic Ocean. It is likely that the strong decay of sea-ice concentration in september since the 2000's show up on the 2000-2007 climatology. On the opposit, after the spin-up phase of few years, the ice concentration remains pretty constant in the climatological run.

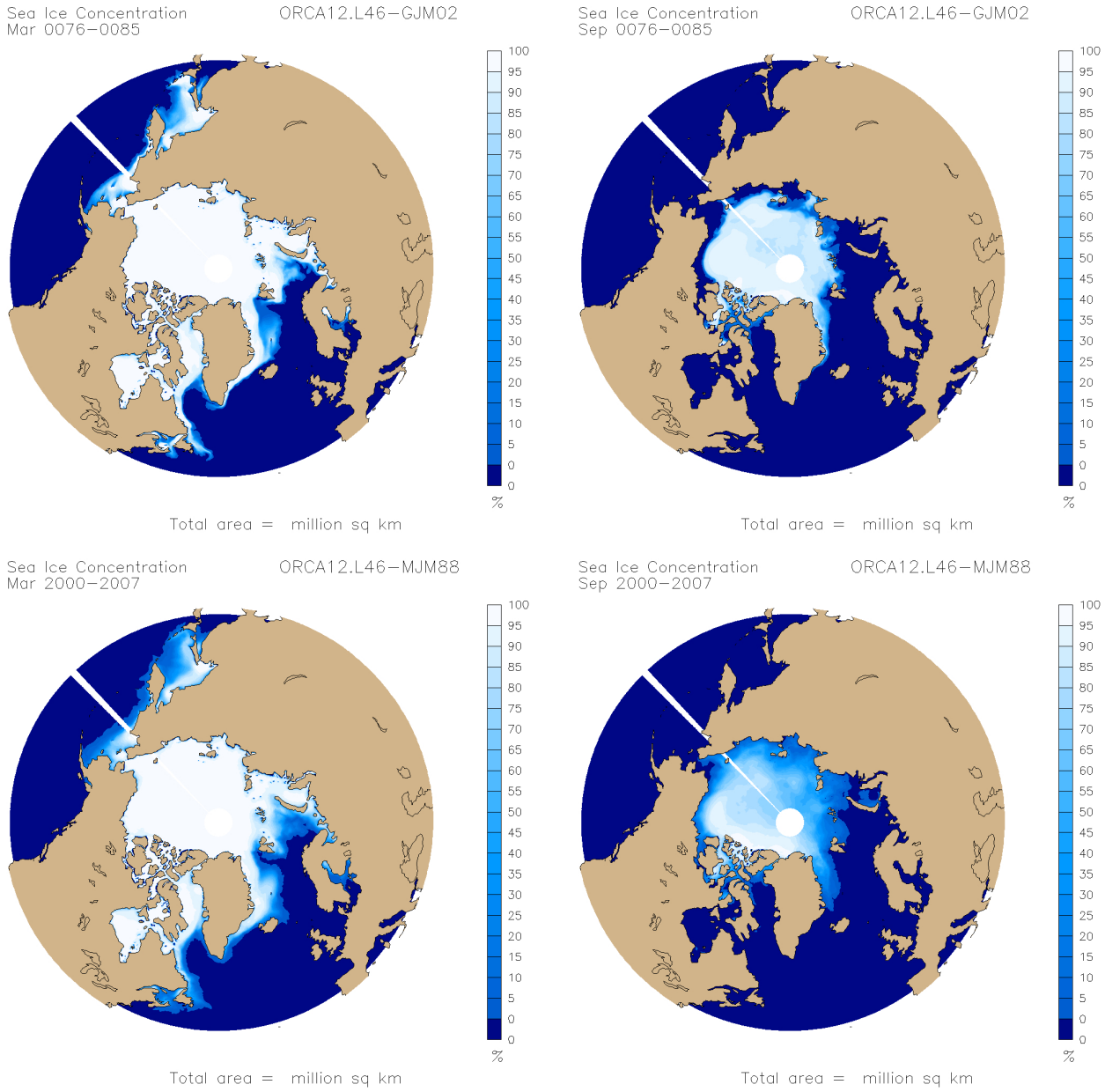

Figure 20: Mean sea-ice concentration in March (left) and September (right) in the Arctic. Top panel for GJM02, bottom panel for MJM88.

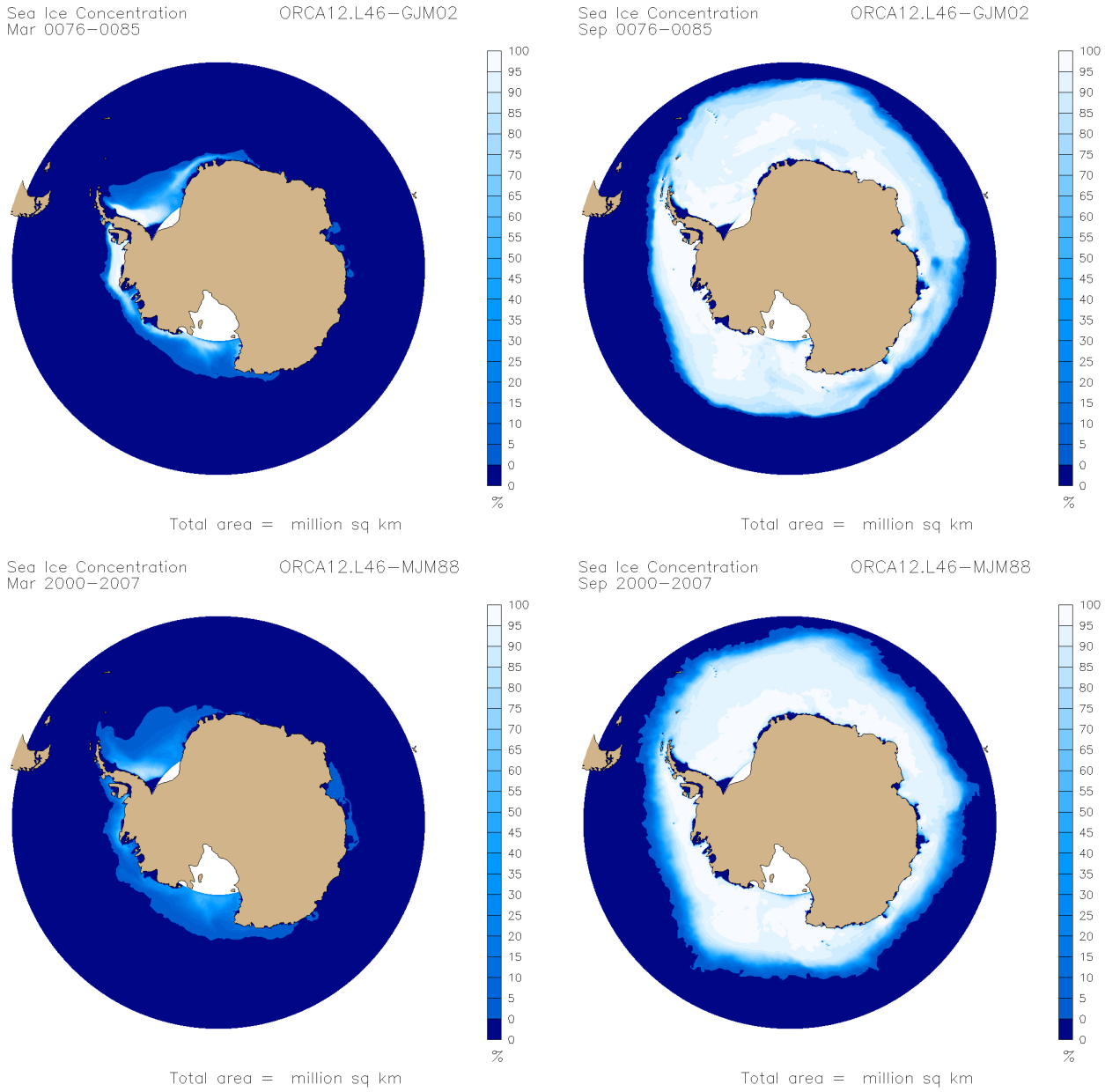

Figure 21: Mean sea-ice concentration in March (left) and September (right) in the Antarctic. Top panel for GJM02, bottom panel for MJM88.

5.5 Variability

5.5.1 Temperature, salinity and SSH drifts

In this section, the global model drifts during the integration is assessed, looking at the time evolution of the 3D average of temperature and salinity as well as the 2D average of the SSH. The vertical profile of temperature and salinity anomalies (*i.e.* differences between final and initial mean profiles) is also computed, as well as its evolution in time. Figure 22 corresponds to the climatological run ORCA12.L46-GJM02 and figure 23 to the interannual run ORCA12.L46-MJM88.

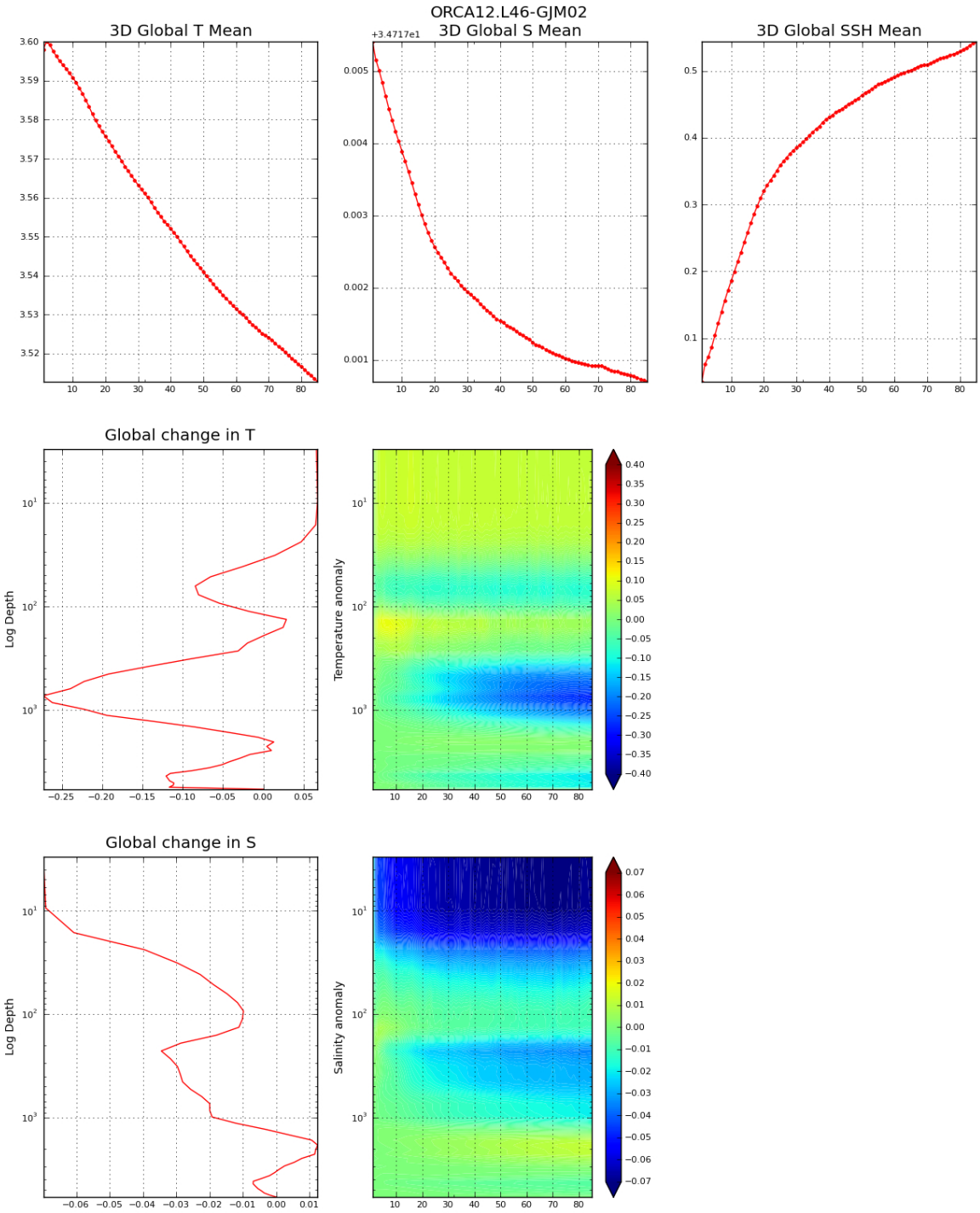

Figure 22: **ORCA12.L46-GJM02**. Top plots: Year-to-year variations of the world ocean average temperature and salinity over the integration period (0001-0085). Middle and bottom plots: Changes compared to initial condition in horizontally averaged temperature and salinity (vertical logarithmic depth range), left is the final minus initial profile, and right is the time evolution of the difference with initial condition.

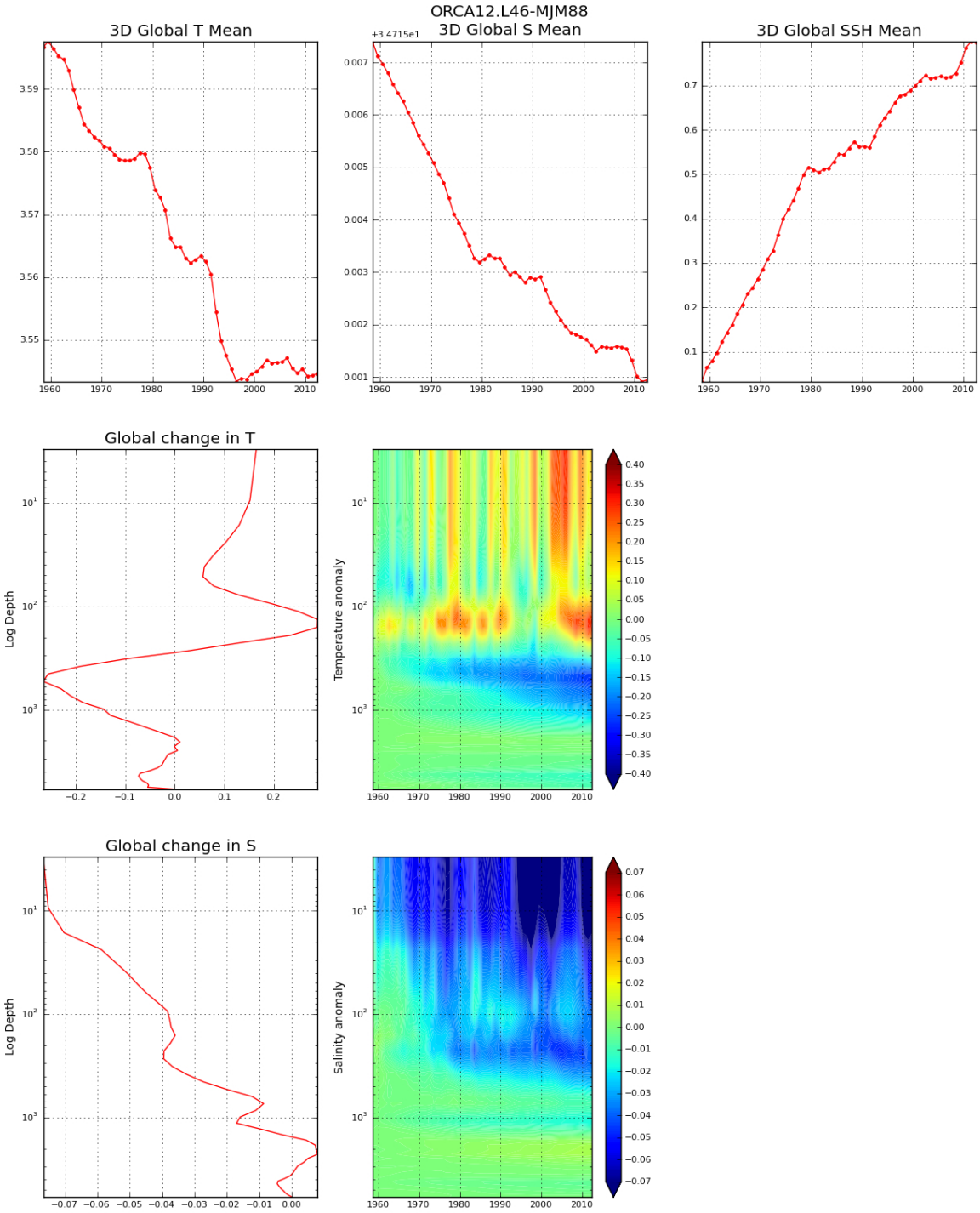

Figure 23: **ORCA12.L46-MJM88**.Top plots: Year-to-year variations of the world ocean average temperature and salinity over the integration period (1958-2012). Middle and bottom plots: Changes compared to initial condition in horizontally averaged temperature and salinity (vertical logarithmic depth range), left is the final minus initial profile, and right is the time evolution of the difference with initial condition.

5.5.2 Overturning and Transport

In this section, two relevant climatic indexes are assessed: the strength of the thermohaline circulation (figure 24) and the Drake passage transport (figure 25). The strength of the thermohaline circulation is estimated by the maximum of the Atlantic overturning circulation. Additionaly, a focus on the Bering strait transport is done (figure 26).

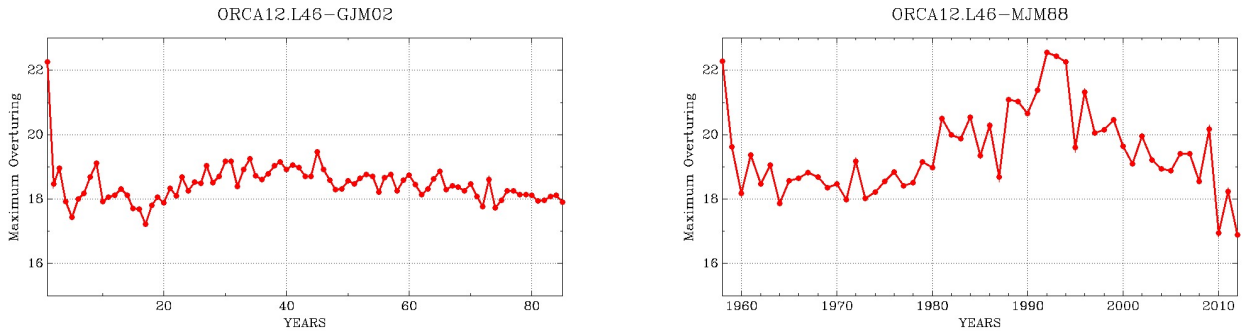

Figure 24: Variations of the annual mean maximum overturning (Sv) in the Atlantic Ocean. Left : GJM02, Right: MJM88.

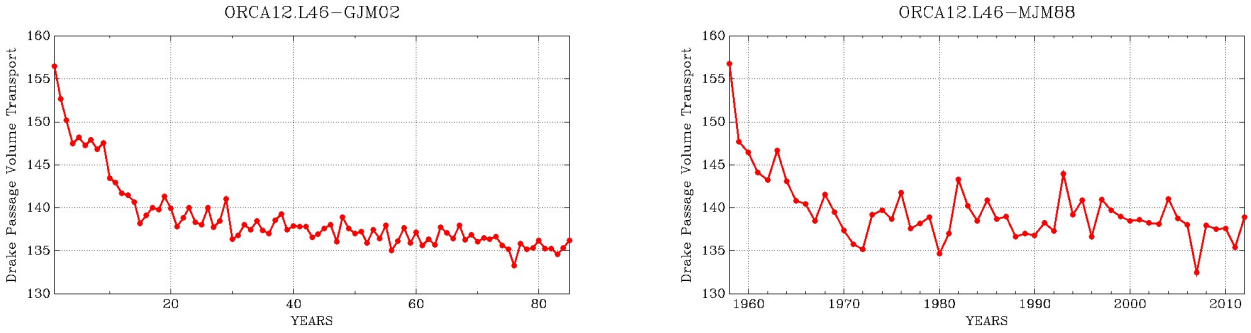

Figure 25: Variations of the annual mean transport (Sv) at Drake passage. Left : GJM02, Right: MJM88.

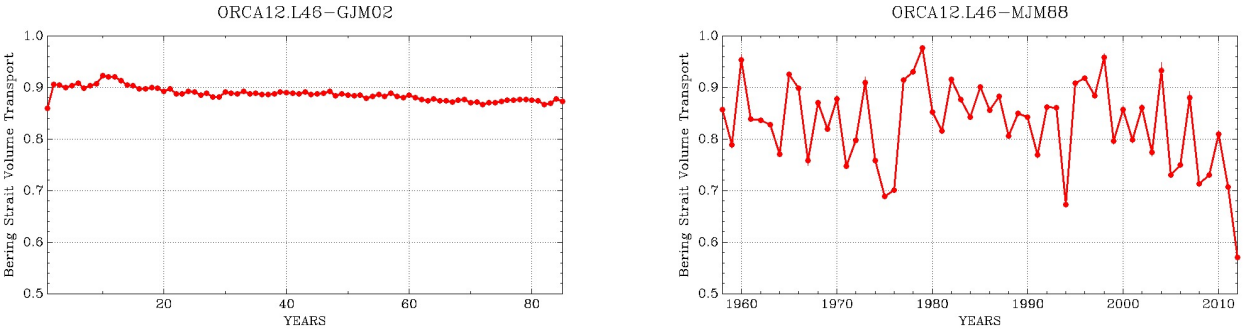

Figure 26: Variations of the annual mean transport (Sv) at Bering Strait. Left : GJM02, Right: MJM88.

5.5.3 Sea-Ice variation CLASS1-3

Model sea ice concentration: 1996 vs 2012: This diagnostic deals with differences in sea ice coverage between two recent summer extrema in the Arctic: the maximum of 1996 and the minimum of 2007. Therefore it is relevant only for the interannual run. Figure 27 shows model results and figure 28 are observations from NSDIC (Fetterer et al., 2002 [8]).

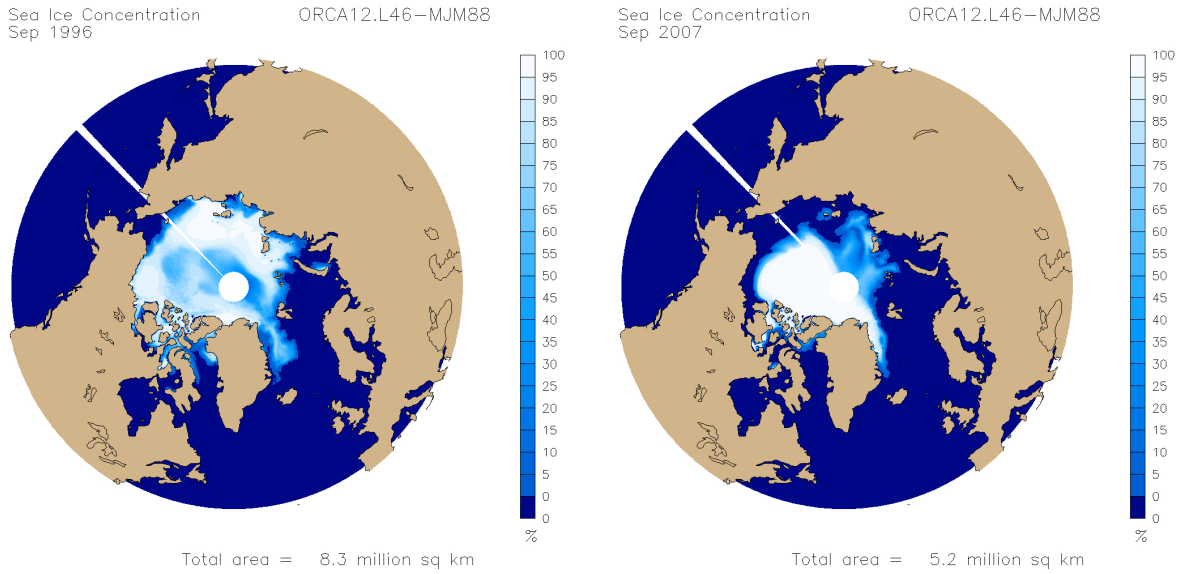

Figure 27: September Sea-Ice Concentration (%) in the Arctic in 1996 (left) and in 2007 (right).

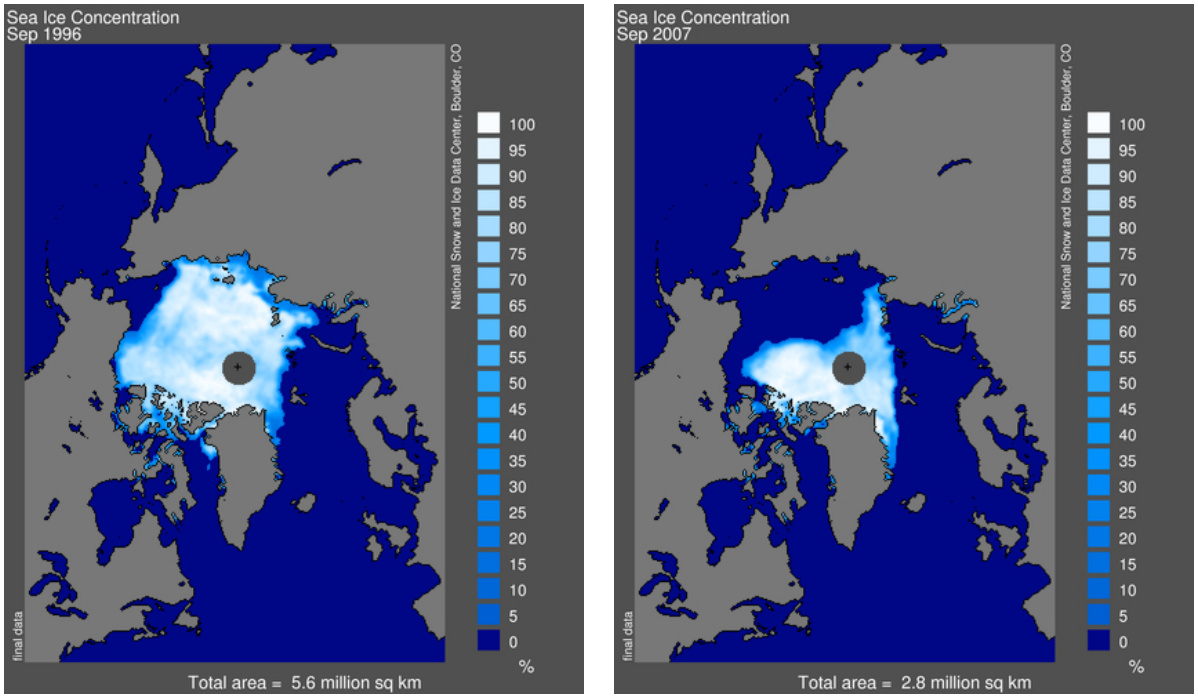

Figure 28: September Sea-Ice Concentration (%) in the Arctic in 1996 (left) and in 2007 (right) from observations available at NSDIC (Fetterer et al., 2002 [8]).

Trend of the minimum ice extent : On the figure 29, the time series of the sea-ice extent for the model (red curve) is compared with satellite based observations (Fetterer et al., 2002

[8], 'blue courve), and it can be seen that the model well capture the decay of the ice-extent in recent years. In particular the extremely low values of year 2007 are in good agreement with observations.

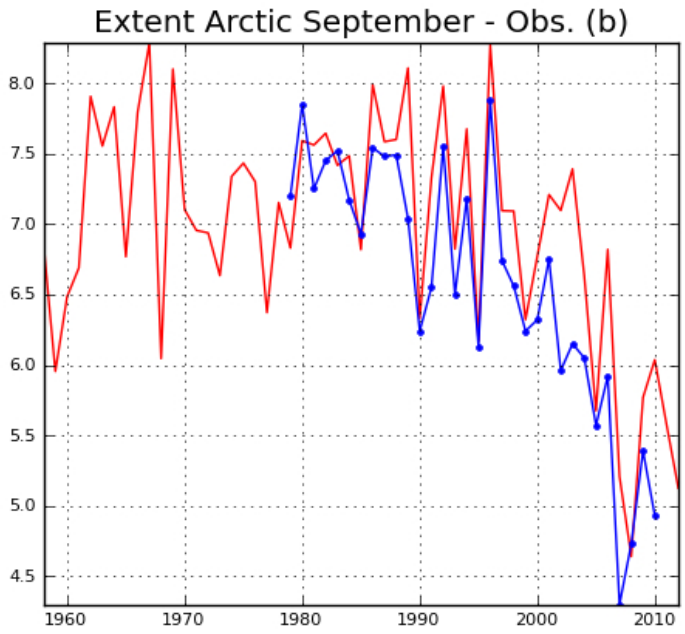

Figure 29: Sea-Ice Extent in September in the Arctic during the integration period (1958-2012). The model results are in red, while satellite observation ([8]) are in blue.

5.5.4 Surface Eddy Kinetic Energy

Eddy kinetic energy represents the variability of the ocean currents. $EKE = \frac{1}{2}(\dot{u'^2} + v'^2)$, where u' and v' are the velocity anomaly with respect to the temporal mean: $u' = (u - \bar{u})$ and $v' = (v - \bar{v})$. On figure 30, the mean value is relative to the model climatology (either 0076-0085 for GJM02 or 2000-2007 for MJM88). Therefore, the interannual variability is captured in this estimate, and not surprisingly EKE is higher for the interannual run. The EKE difference between the two experiments can be interpreted as the forced part of the EKE (by opposition to the intrinsic part). Penduff et al (2011)[20] analysed a similar pair of experiments with ORCA025 in order to un-ravel the intrinsic variability of the ocean.

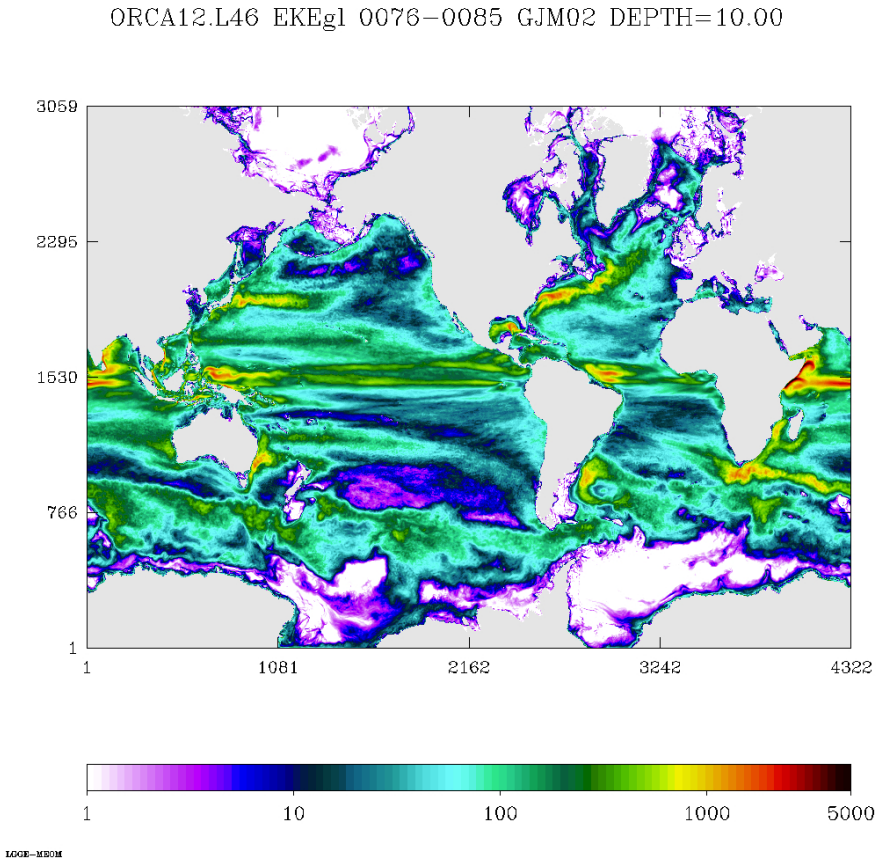

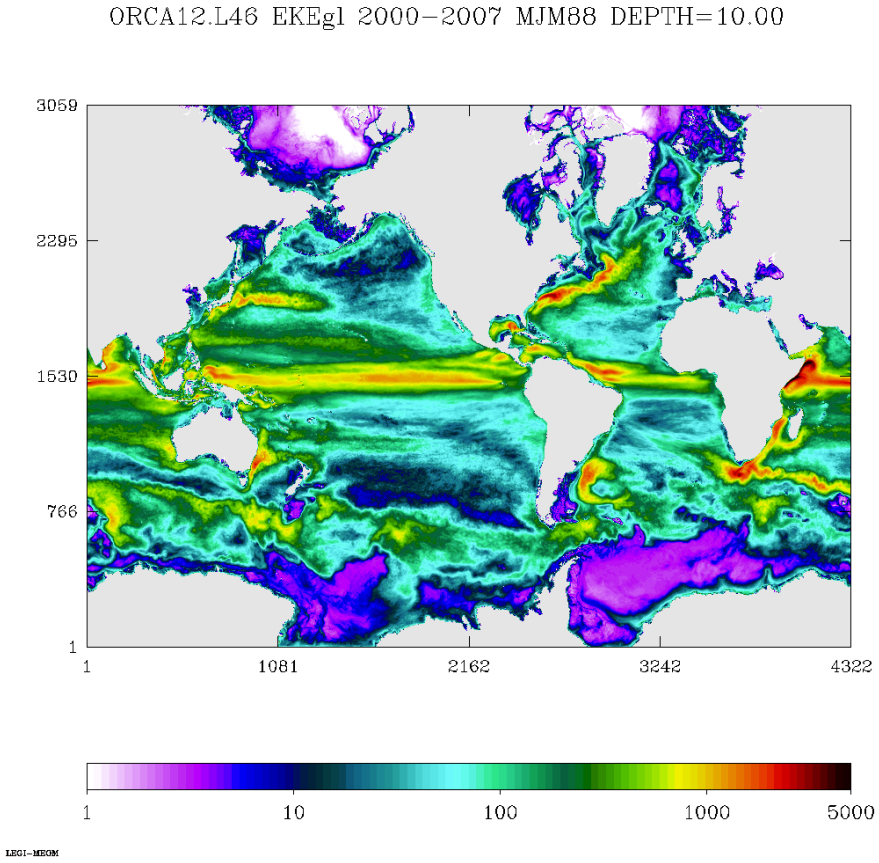

Figure 30: Surface EKE for GJM02 (left) and MJM88(right). Units are cm^2/s^2.

5.5.5 El Nino

This section concerning El Niño, is only relevant for the interannual run ORCA12.L46-MJM88. This diagnostic, compare mean SST, computed in predefined boxes (figure 31) with observed mean SST computed in the same boxes. On figure 32, the model SST is shown in red, the observations in blue. Except for box Ninõ 1+2, where a warm bias is observed, the correspondance model-observations is remarkable for all other boxes. The warm bias results from the a too weak upwelling in the model.

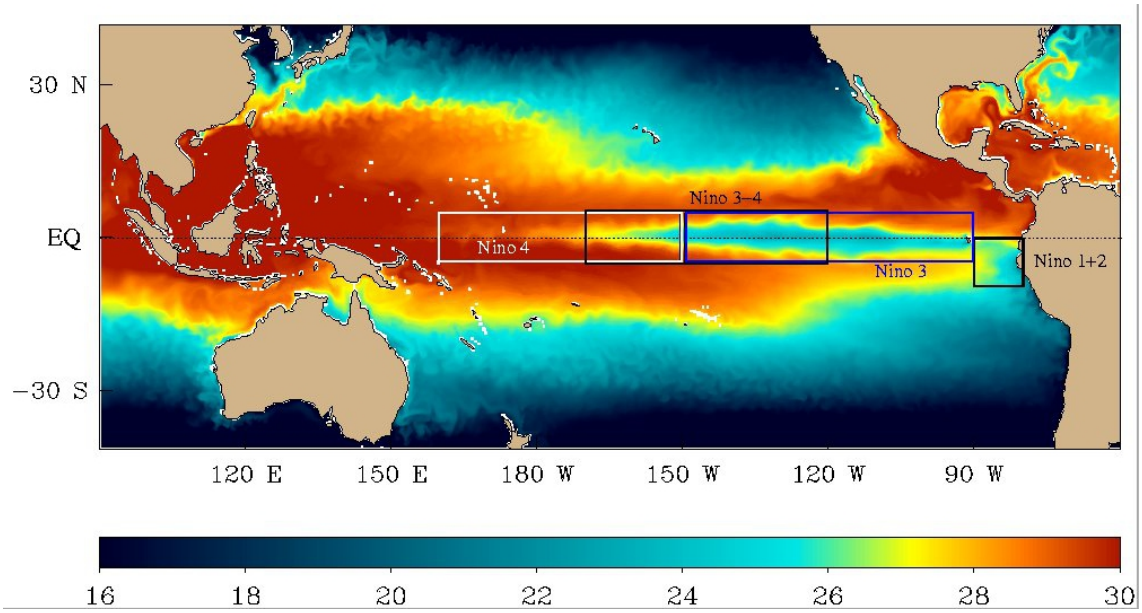

Figure 31: Definition of the Nino boxes. Background colors represent the instantaneous SST of a previous ORCA025 run.

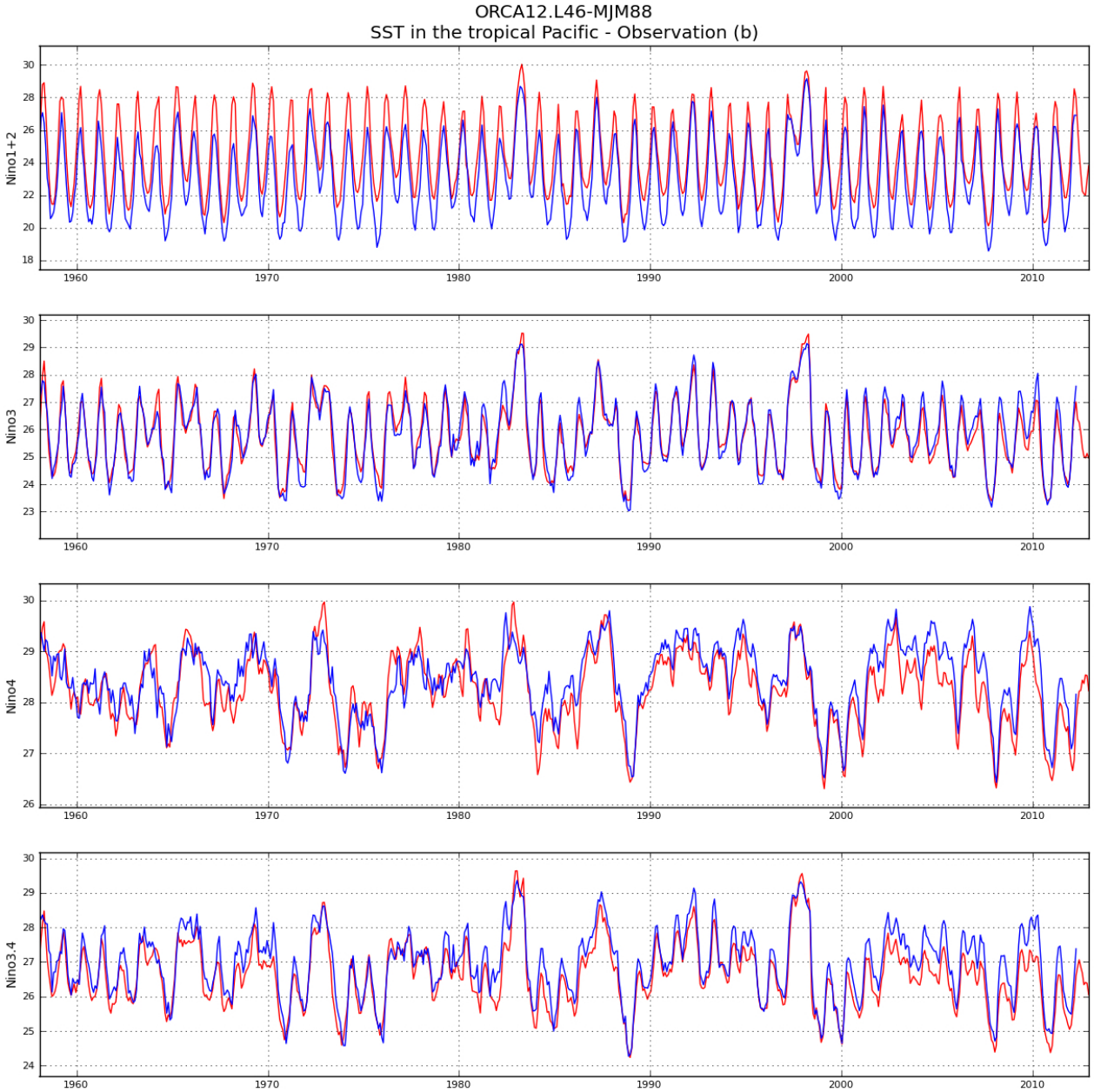

Figure 32: Monthly mean variations of the average temperatures in el Nino boxes. Red curves are model SST, blue curves are observations.

Acknowledgement

ORCA12.L46-GJM02 has been performed on 'ada' super computer (IDRIS), as one of the 'Grands Challenges' organized during the reception period of the computer. ORCA12.L46-MJM88 has been performed on 'jade' supercomputer (CINES) with regular CPU hours allocated by GENCI Grant X2013-90727.

References

[1] A. Beckmann and R. Döscher. A method for improved representation of dense water spreading over topography in geopotential-coordinate models. *J. Phys. Oceanogr.*, 27:581–

591, 1997.

[2] L. Bessiéres, G. Madec, and F. Lyard. Global tidal residual mean circulation: Does it affect a climate ogcm? *Geophys. Res. Let.*, 35:L03609, 2008.

[3] R. Bourdallé-Badie, A.-M. Treguier, J.-M. Molines, A. Coward, M. Scheinert, Y. Lu, A. Lecointre, and B. Tranchant. The ORCA12 bathymetry V3.2. Technical report, MERCATOR-DRAKKAR report, 2012.

[4] L. Brodeau, B. Barnier, A.-M. Tréguier, T. Penduff, and S. Gulev. An era40-based atmospheric forcing for global ocean circulation models. *Ocean Modelling*, 31(3-4):88–104, 2009.

[5] E. Dai and K.E. Trenberth. Estimates of freshwater discharge from continents: Latitudinal and seasonal variations. *J. Hydrometeorology*, 3:660–687, 2002.

[6] C.O Dufour. *Rôle des tourbillons océaniques dans la variabilité récente des flux air-mer de CO2 dans l'océan Austral (Impact of oceanic eddy activity on the variability of CO2 air-sea fluxes in the Soutthern Ocean).* PhD thesis, Université de Grenoble, France, 2011.

[7] C.O Dufour, J. Le Sommer, J.D. Zika, M. Gehlen, J.C. Orr, P. Mathiot, and B. Barnier. Standing and transient eddies in the response of the southern ocean meridional overturning to the southern annular mode. *J. Climate*, 25(12):6958–6974, 2012.

[8] F. Fetterer, K. Knowles, and M. Savoie. Sea Ice Index. Technical report, Boulder, Colorado USA: National Snow and Ice Data Center. Digital media, 2002.

[9] G. Hervieux. *Etude numérique des interactions courant-topographie: applications au gyre subpolaire, aux seuils de Gibraltar et des mers nordiques.* PhD thesis, Université J. Fourier, Grenoble, 2007.

[10] A. Koch-Larrouy, G. Madec, P. Bouruet-Aubertot, T. Gerkema, L. Bessieres, and R. Molcard. Tidal mixing in the indonesian seas and its effect on the tropical climate system. *Geophys. Res. Let.*, 34:L04604, 2007.

[11] W. G. Large and S. Yeager. *Diurnal to decadal global forcing for ocean and sea-ice models: the data sets and flux climatologies.* NCAR Technical Note, NCAR/TN-460+STR, CGD Division of the National Center for Atmospheric Research, 2004.

[12] A. Lecointre. Influence of solver on NEMO3.4 ORCA12 performance and scalability on SGI JADE (GENCI-CINES) supercomputer. Technical report, LEGI-CNRS, Grenoble, France, LEGI-DRA-2012-05-04, 2012.

[13] A. Lecointre. NEMO3.4 performance tests with ORCA12.L46 on JADE (GENCI-CINES) supercomputer. Technical report, LEGI-CNRS, Grenoble, France, LEGI-DRA-2012-04-17, 2012.

[14] A. Lecointre, J.-M. Molines, and N. Audiffren. Tests de performance d'un modèle océanographique haute résolution sur le supercalculateur parallèle JADE (GENCI-CINES). Poster (a more detailed technical report is in preparation), HPC GENCI, May 19th, Paris, 2011.

[15] A. Lecointre, J.-M. Molines, and B. Barnier. Definition of the interannual/climatological experiment ORCA12.L46-MAL101, 1979-2010. Technical report, LEGI-CNRS, Grenoble, France, LEGI-DRA-2012-07-xx, 2012.

[16] M. Lengaigne, C. Menkes, O. Aumont, T. Gorgues, L. Bopp, J.-M. André, and G. Madec. Bio-physical feedbacks on the tropical pacific climate in a coupled general circulation model. *Clim. Dyn.*, 28:503–516, 2007.

[17] G. Madec. *NEMO ocean engine.* Note du Pôle de modélisation, Institut Pierre-Simon Laplace (IPSL), France, No 27, ISSN No 1288-1619, 2008.

[18] P. Mathiot. *Influence du forçage atmosphérique sur la représentation de la glace de mer et des eaux de plateau en Antarctique dans une étude de modélisation numérique.* PhD thesis, Université de Grenoble, France, 2009.

[19] A. Melet, J. Verron, L. Gourdeau, and A. Koch-Larrouy. Solomon sea water masses pathways to the equator and their transformations. *J. Phys. Oceanogr.*, 41:810–826, 2011.

[20] T. Penduff, M. Juza, B. Barnier, J. Zika, W.K. Dewar, A.M. Treguier, J-M. Molines, and N. Audiffren. Sea level expression of intrinsic and forced ocean variabilities at interannual time scales. *J. Climate*, 24:5652–5670, 2011.

[21] Dussin R., B. Barnier, and L. Brodeau. The Making of DFS . Technical report, LGGE-CNRS, Grenoble, France, GDRI DRAKKAR 2014-001, 2014.

[22] T. A. M. Silva, G. R. Bigg, and K. W. Nicholls. Contribution of giant icebergs to the southern ocean freshwater flux. *J. Geophys. Res*, 111(C03004):1–8, 2006.

[23] A. M. Treguier, J. Deshayes, J. Le Sommer, C. Lique, G. Madec, T. Penduff, J.-M. Molines, and B. Barnier. Meridional transport of salt in the global ocean from an eddy-resolving model. *Ocean Sc.*, 3:in press, 2014.